MEMBRANE SEPARATIONS

RATE CONTROLLED SEPARATION PROCESSES

ETH ZURICH — HS 2016

Department of Mechanical and Process Engineering

Prof. Dr. Marco Mazzotti

Dr. Matteo Gazzani

Federico Milella

Paolo Gabrielli

October 7, 2016

ETH
Eidgenössische Technische Hochschule Zürich
Swiss Federal Institute of Technology Zurich

Note for students — HS 2016

For the preparation of the exam the following parts of the script are of less importance:

- section 1.3;
- eqs. (1.11), (1.12) and (1.16);
- chapter 2.

The analysis of section 3.3 and 3.4 should be limited to what has been done during the lecture.

Contents

SYMBOLS

Latin Letters		
A	Total membrane area	m^2
a	Activity coefficient	-
c	Molar concentration	$\mathrm{mol}/\mathrm{m}^3$
D	Diffusion coefficient	m^2/s
$Đ$	Maxwell-Stefan diffusion coefficient	m^2/s
f_α	Fugacity of component α	Pa
$\bar{J}$	Molar flux across the membrane	mol/(m^2 s)
K_s	Sorption coefficient	${\mathrm{m}_i}^3/{\mathrm{m}_m}^3$
K	Darcy permeability coefficient	mol / (m^2 Pa s)
L	Membrane module length	m
M	Molar weight	kg/kmol
N_c	Number of components	-
$\dot{n}$	Molar flow rate	mol/s
P	Product purity	-

p	Total pressure	Pa
p_i	Partial pressure of component i	Pa
p^*_α	Vapor pressure of component α	Pa
Q	Membrane permeability	mol/(m s Pa)
R	Product recovery	-
r	Radius	m
s	Surface	m^2
T	Temperature	K
$\bar{v}$	Velocity	m/s
$\hat{v}$	Specific volume	m^3/kg
$\tilde{v}$	Molar volume	m^3/mol
W	Membrane module width	m
x	Molar fraction in liquid phase	mol/mol
y	Molar fraction in gas phase	-
z	Axial coordinate	m
Greek Letters		
α	Membrane selectivity	-
α^*	Separation factor	-
β	Permeate to retentate pressure ratio	-
γ	Retentate to permeate pressure ratio	-
δ	Membrane thickness	m
π	Osmotic pressure	Pa
σ	Dimensionless membrane area coordinate	-
θ	Stage cut	-
Φ	Dimensionless membrane flux	-
ϕ	Electric potential	V
ψ	Dimensionless retentate mole flow	-
ω	Dimensionless permeate mole flow	-
Subscripts		
i	Component i	
F	Feed stream	
m	Membrane	
P	Permeate stream	
R	Retentate stream	
Superscripts		
I	Membrane interface	

CHAPTER 1

MEMBRANES THEORY

1.1 Introduction

A generic separation process of a mixture can be achieved applying different technologies e. g. distillation, adsorption, absorbtion or membranes. Each technology features its own transport equations but from an overall point they can be regarded as similar/competitive solutions to separate a generic (A,B) mixture into A and B. A

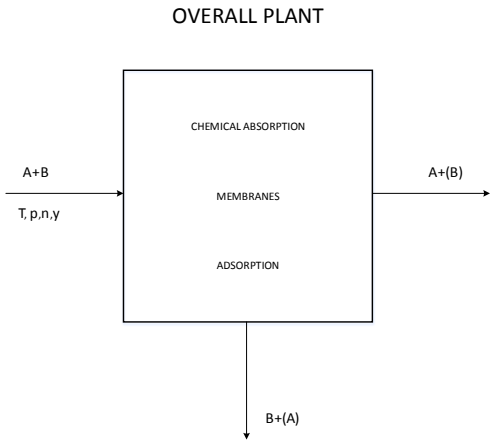

Figure 1.1: Generic process overview

membrane is a selective barrier that allows the passage of certain components and retains others in the liquid or gas mixture. The stream that enters the membrane is called feed-stream, the fluid that passes through the membrane is known as the permeate while the fluid that contains the retained components is named retentate or concentrate. Membranes can therefore be assembled into modules in order to perform a separation process that achieves the desired process specifications.

1.2 Mass Balances Over A Membrane Module

By considering a control volume that includes the whole membrane module it is possible to impose the total and single species mass balance constraints.

Overall mass balance (hyp.: no chemical reactions)

$$\dot{n}_f = \dot{n}_p + \dot{n}_r = \sum_i \dot{n}_f x_{i,f} = \sum_i \dot{n}_p x_{i,p} + \sum_i \dot{n}_r x_{i,r} \tag{1.1}$$

where,

- $\dot{n}_f$, is the total molar flow-rate in the feed stream;
- $\dot{n}_p$ is the total molar flow-rate in the permeate stream;
- $\dot{n}_r$ is the total molar flow-rate in the retentate stream;
- x_i is the molar fraction of component i.

Single species overall mass balance

$$\dot{n}_f x_{i,f} = \dot{n}_p x_{i,p} + \dot{n}_r x_{i,r} \tag{1.2}$$

which is complemented by the closure constraint on molar fractions for each process stream:

$$\sum_i x_{i,f} = \sum_i x_{i,r} = \sum_i x_{i,p} = 1 \tag{1.3}$$

By considering a control volume that includes the whole membrane module it is possible to frame the total mass flux across the membrane into the mass balance

$$\dot{n}_f = \dot{n}_r + \dot{n}_p = \dot{n}_r + \int_A J dA \tag{1.4}$$

where,

- $J = \sum J_i$ is the total molar flux of permeating species;
- J_i represents the molar flux equation for species i across the membrane;
- A represents the membrane section area where mass transfer occurs.

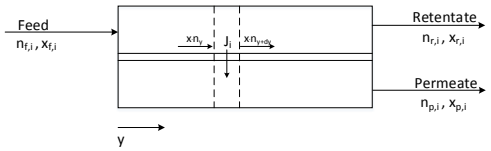

Figure 1.2: Mass balance over a membrane module.

In order to quantitatively solve the membrane mass balance equations it is convenient consider a local approach. The local separation process can be described by choosing an infinitesimally small arbitrary control volume within the membrane. The single species mass balance holds:

$$(x_{i,r}\dot{n}_r)|_y - (x_{i,r}\dot{n}_r)|_{y+dy} = J_i dA \tag{1.5}$$

Figure 1.2 resembles a local section of a membrane module. Through the use of this scheme it is possible to define the input data which represents the design specifications (e. g. feed flow rate, composition and operative conditions), as well as the output variables (e. g. membrane area) involved in the process.

It is therefore necessary to develop mathematical models able to describe each generic flux through the membrane as a function of the physical variables of the system.

1.3 Description of mass transfer across selectively permeable membranes

Mass transport across membranes involves different driving forces. The wide range of behavior resulting from these various driving forces can be described compactly via the framework provided by non-equilibrium thermodynamics (NET). NET makes use of four postulates above and beyond those of equilibrium thermodynamics:

- the equilibrium thermodynamic relations apply to systems that are not in equilibrium, provided that gradients are not too large (local equilibrium);
- all fluxes in the system may be written as linear relations involving all the driving forces;
- no coupling of fluxes and forces occurs if the difference in tensorial order of the flux and force is an odd number (Curie's Postulate);
- in the absence of magnetic fields, the matrix of the coefficients in the flux-force relations is symmetric (Onsager's reciprocal relations).

The description of mass transfer when multiple driving forces are present is given by the Maxwell-Stefan equations. Eventhough the derivation of these equations is not in the scope of this script, it is important to understand how these equations are derived:

- the starting point for derivation of Maxwell-Stefan equations is the entropy-balance equation for irreversible processes (entropy remains a valuable state function in non-equilibrium under the local equilibrium assumption).

Entropy balance

$$\rho \frac{D\hat{S}}{Dt} = -(\nabla \cdot \bar{J}_s) + g_s \tag{1.6}$$

where,

- ρ is the density of the mixture;
- $\bar{J}_s$ is the entropy flux vector;
- g_s is the entropy generation per unit volume.

A lagrangian approach is used where the evolution of a specific control volume element is followed in time.
The derivation of the entropy balance follows

$$\frac{DS}{Dt} = \underbrace{\frac{dS|_e}{dt}}_{\text{Rate of exchange with exterior}} + \underbrace{\frac{dS|_i}{dt}}_{\text{Rate of internal production}}$$

Appling the divergence theorem over a generic control volume of surface Σ ($\int_V \nabla \cdot \bar{F}\, dV = \oint_{\partial V} \bar{F} \cdot d\bar{S}$)

$$\int_V \rho \frac{D\hat{S}}{Dt} = -\int_\Sigma \bar{J}_s \cdot \bar{n}\, d\Sigma + \int_V g_s\, dV = -\int_V \nabla \cdot \bar{J}_s\, dV + \int_V g_s\, dV$$

Due to the arbitrary chosen control volume the local balance, eq. 1.6, is obtained equating the arguments of the integrals.
By using the conservation laws for mass, momentum and energy, together with the equilibrium relation $dU = TdS - pdV + \sum_i \frac{\mu_i}{M_i} dn_i$, it is possible to express the entropy flux $\bar{J}_s$ and entropy generation g_s as a sum of products of fluxes and forces (g_s) or sum of fluxes ($\bar{J}_s$).
The result of this procedure brings to the Maxwell-Stefan generalized equations:

$$\begin{aligned}\nabla x_\alpha = \sum_{\beta=1}^{N\neq\alpha} \frac{x_\alpha x_\beta}{Đ_{\alpha\beta}}(\bar{v}_\alpha - \bar{v}_\beta) = & \underbrace{-x_\alpha \nabla \ln a_\alpha}_{\text{Concentration diffusion term}} + \\ & - \frac{1}{cRT}\left[\underbrace{(\phi_\alpha - \omega_\alpha)\nabla p}_{\text{Pressure diffusion term}} \underbrace{-\rho_\alpha \bar{g}_\alpha + \omega_\alpha \sum_{\beta=1}^{N} \rho_\beta \bar{g}_\beta}_{\text{Forced diffusion term}}\right] + \\ & \underbrace{- \sum_{\beta=1}^{N\neq\alpha} \frac{x_\alpha x_\beta}{Đ_{\alpha\beta}} \left(\frac{D_\alpha^T}{\rho_\alpha} - \frac{D_\beta^T}{\rho_\beta}\right) \nabla T}_{\text{Thermal diffusion term}}\end{aligned} \tag{1.7}$$

where,

- $Đ_{\alpha\beta}$ are the Maxwell-Stefan diffusivities;
- D_i^T is the thermal diffusivities of component i.

For binary diffusion in gases or liquids

$$\begin{aligned}\bar{J}_\alpha = c Đ_{\alpha\beta} \nabla x_\alpha = -c Đ_{\alpha\beta} \Bigg[& x_\alpha \nabla \ln a_\alpha + \\ & + \frac{1}{cRT}\left((\phi_\alpha - \omega_\alpha)\nabla p - \rho \omega_\alpha \omega_\beta (\bar{g}_\alpha - \bar{g}_\beta)\right) + k_T \nabla \ln T \Bigg]\end{aligned} \tag{1.8}$$

The contribution of external forces (gravity field, electrostatic field and mechanical forces) can be written as

$$\bar{g}_\alpha = \bar{g} - \frac{z_\alpha F}{M_\alpha} \nabla \phi + \delta_{\alpha,m} \frac{1}{\rho_m} \nabla p \tag{1.9}$$

The term $\delta_{\alpha,m}\frac{1}{\rho_m}\nabla p$ represents the mechanical constraint that keeps the membrane stationary against external pressure gradients and internal viscous drag (typically a wire mesh or equivalent structure is used).
Membranes consist of an insoluble, selective permeable matrix m and one or more permeating species α, β.
The following constraints hold:

- negligible curvature: $\delta << \mathrm{R_{curv}}$ (mass transport in unidirectional and perpendicular to the membrane surface);
- immobility of the matrix: $v_m = 0$;
- pseudosteady behaviour: $\frac{\partial c_\alpha}{\partial t} = 0$ (diffusional terms within the membrane are short compared to those in the adjacent solution;
- no thermal diffusion.

It follows that the Maxwell-Stefan equations can be slightly simplified:

- the term $\omega_\alpha \nabla p$ can be set to zero as the membrane is stationary;
- the thermal diffusion term can be neglected;
- since the membrane is, to an excellent approximation, incompressible and of uniform chemical composition, the equivalent body force will be uniform and of magnitude $\bar{g} = \frac{1}{\rho_m}\nabla p$.

The resulting Maxwell-Stefan equation can be therefore written as:

$$\begin{aligned}\sum_{\beta=1}^{N}\frac{RT}{Đ_{\alpha\beta}c}(x_\beta \bar{N}_\alpha - x_\alpha \bar{N}_\beta) = \\ = -x_\alpha RT\nabla \ln a_\alpha - z_\alpha F\nabla V + \left(\frac{\delta_{\alpha,m}}{\rho_m} - \bar{V}_\alpha\right)\nabla p\end{aligned} \tag{1.10}$$

where $\bar{N}_\alpha$ and $\bar{N}_\beta$ represent the molar fluxes, $\delta_{\alpha,m}$ the Kronecker delta and $\bar{V}_\alpha$ the partial molar volume of α.

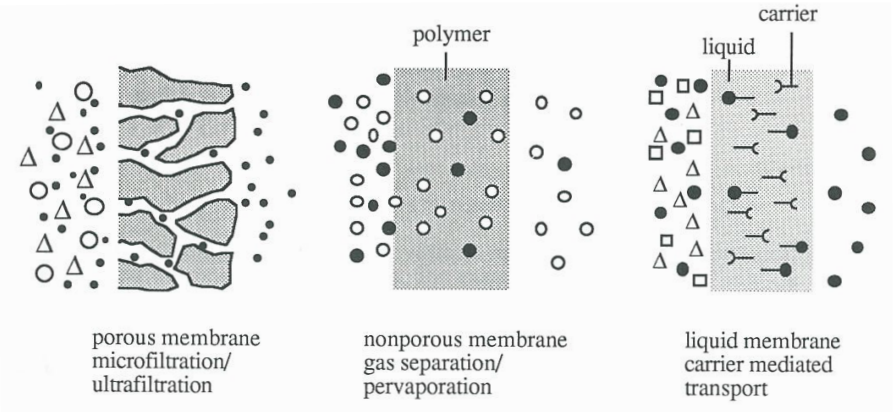

Figure 1.3: Schematic representation of the basic types of membrane

Along with the Maxwell-Stefan equation for membrane transport, a generally applicable set of boundary conditions has to be defined: these conditions are obtained by requiring the "total potential" of each species to be continuous across the boundary of the membrane and the solution bathing the membrane (local equilibrium). Since conditions within the membrane are very difficult, or even impossible, to determine, this equation is primarly useful to obtain a qualitative understanding of membrane behavior. What is the way to proceed then? The approach is to use simplified models (based on the Maxwell-Stefan equation introducing simplifications) that allow to describe a membrane quantitatively with a good agreement with respect to experimental data. The model will be therefore simplified according to the type of membrane considered. There are many transport mechanisms involved depending on the type of selective barrier:

- *porous membranes*[1] (mean pore size diameter 5000 - 1 nm)
  In porous membranes molecules are transported by a pressure-driven convective flow through tiny membrane pores (pores size bigger that 10^{-9} m). A difference in steric hindrances between the components' molecules and the membrane material leads therefore to different compounds permeabilities. The permeant concentration within a porous membrane is uniform and the only driving force across the membrane is the pressure gradient.

- *homogeneous membranes*[1] (mean pore size diameter less than 1 nm)
  In dense membranes molecules of the different compounds first dissolve into the membrane matrix and then diffuse through the membrane under a concentration gradient. The permeability of each species is therefore affected by the solubil-

[1]Considered in rate controlled separation processes class

ity of each compound into the membrane material (thermodynamic aspect) and by the rate at which each component diffuses through the membrane (kinetics aspect).The average pore diameter in dense polymer membranes is within the thermal motion of the polymer chains from which the membrane is made of.

- *facilitated diffusion/charged membranes*
  In a carrier-mediated diffusion membrane the movement of molecules across the membrane occurs via very specific carrier-molecules that are embedded within the membrane. The permselectivity towards a component depends mainly on the specificity of the carrier molecule. Through the use of specially tailored carriers, extremely high selectivities can be obtained. The component to be removed can be gaseous or liquid, ionic or non-ionic. To some extent the functionality of this kind of membranes approaches that of a cell.

- *active transport*
  In membranes where active transport occurs the movement of molecules (against some concentration gradients or other form of resistance) across the membrane requires energy. Unlike passive transport, which uses natural entropy of molecules moving down a gradient, active transport uses external sources of energy (electrochemical gradients, etc.) to perform a separation.

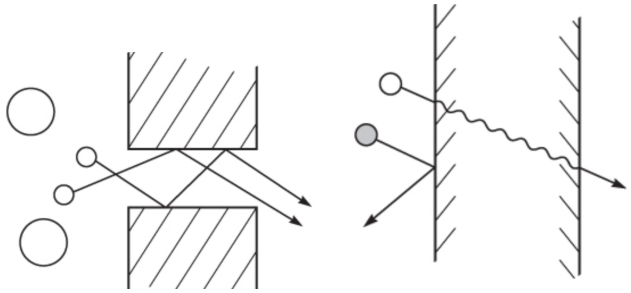

(a) *Microporous membranes separate by molecular filtration.*

(b) *Dense solution-diffusion membranes separate because of differences in the solubility and mobility of permeants dissolved in the membrane material.*

Figure 1.4: Membranes mass transfer models

1.4 Models For Mass Transfer Through Membranes

Two basic models[2] for mass transfer through the membrane will be considered:

- the hydrodynamic model for porous membranes;
- the solution-diffusion model for dense membranes.

Through a manipulation of the simplified Maxwell-Stefan equation (eq. 1.10) it is possible to express the molar flux of component α as:

$$\bar{N}_\alpha = \bar{J}_\alpha = -c\text{Đ}_{\alpha\beta}\left[x_\alpha \nabla \ln a_\alpha + \frac{1}{cRT} c_\alpha \bar{v}_\alpha \nabla p - \rho_\alpha \bar{g}_\alpha + \omega_\alpha \sum_{\beta=1}^{N} \rho_\beta \bar{g}_\beta\right] \quad (1.11)$$

In the case of binary mixtures the left term in eq. 1.10 can be written as

$$\sum_{\beta=1}^{N} \frac{1}{D_{\alpha\beta} c}(x_\beta \bar{N}_\alpha - x_\alpha \bar{N}_\beta) = \frac{1}{D_{\alpha\beta} c}\bar{N}_\alpha = -\frac{1}{D_{\alpha\beta} c}\bar{N}_\beta \quad (1.12)$$

due to the fact that $x_\alpha + x_\beta = 1$ and $\bar{N}_\alpha + \bar{N}_\beta = \bar{0}$.

[2] J. G. Wijmans, R. W. Baker, The solution-diffusion model: a review, Journal of Membrane Science 107 (1995) 1-21.

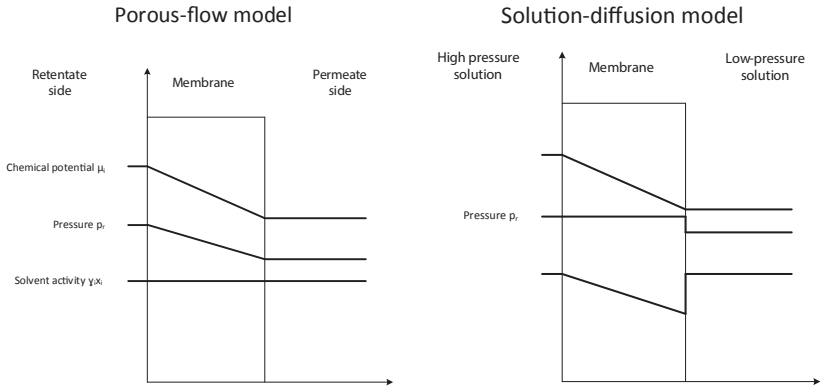

(a) *Porous-flow model*. (b) *Solution-diffusion permeation model*.

Figure 1.5: Comparison between the hydrodynamic permeation and solution-diffusion permeation models for mass transfer through the membrane.

1.4.1 Pore-flow (hydrodynamic) Model

In the framework of porous membranes the mass transport mechanism is model as a pure convective motion of molecules across the membrane due to a superimposed pressure gradient. Eq. 1.11 can be reconsidered in light of the simplification introduced by this model.

$$\bar{J}_\alpha = -c\text{Đ}_{\alpha\beta}\left[\frac{1}{cRT}c_\alpha \bar{v}_\alpha \nabla p - \rho_\alpha \bar{g}_\alpha\right] \tag{1.13}$$

It follows that

$$\bar{J}_\alpha = -\frac{\text{Đ}_{\alpha\beta}}{RT}\bar{v}_\alpha c_\alpha \nabla p = -c_\alpha K^{'}\frac{dp}{dz} \tag{1.14}$$

Eq. 1.14 is named Darcy equation where the following terms represents

- $\frac{dp}{dz}$: pressure gradient;
- c_α: concentration of component A in the medium;
- $K^{'}$: permeability of the medium.

1.4.2 Solution-Diffusion Model

In the solution-diffusion model, transport occurs only by diffusion. The component that needs to be transported must first dissolve in the membrane.
The molar flux of component α can be therefore expressed using eq. 1.10

$$\bar{J}_\alpha = -c\text{Đ}_{\alpha\beta}x_\alpha \nabla \ln a_\alpha \tag{1.15}$$

since

- no pressure gradient exists within the membrane;
- no external forces act on the membrane.

In the solution-diffusion model, the pressure within the membrane is constant at the high-pressure value (p_r), and the gradient in chemical potential across the membrane is expressed as a smooth gradient in solvent activity ($\gamma_s x_s$) as shown in fig. 1.5.
By introducing the definition of activity, $a_\alpha = \gamma_\alpha x_\alpha$, in eq. 1.15

$$\bar{J}_\alpha = -c\text{Đ}_{\alpha\beta}\left(\frac{\partial \ln a_\alpha}{\partial \ln x_\alpha}\right)_{T,p} \nabla x_\alpha = -c\text{Đ}_{\alpha\beta}\left[1 + \left(\frac{\partial \ln \gamma_\alpha}{\partial \ln x_\alpha}\right)_{T,p}\right] \nabla x_\alpha \quad (1.16)$$

Under the hypothesis of perpendicular flux it is possible to write

$$\bar{J}_\alpha = -cD_{\alpha,\beta}\nabla x_\alpha = -cD_{\alpha,\beta}\frac{dx_\alpha}{dz}\hat{n} \quad (1.17)$$

where,

- $D_{\alpha,\beta} = \text{Đ}_{\alpha\beta}$ for an ideal mixture;
- $D_{\alpha,\beta} = \text{Đ}_{\alpha\beta}\left[1 + \left(\frac{\partial \ln \gamma_\alpha}{\partial \ln x_\alpha}\right)_{T,p}\right]$ for a non-ideal mixture.

Eq. 1.17 is the simplified Fick equation with diffusivities accounting for mixtures non-ideality.

The flux equations respectively for porous membranes and homogeneous membranes have been obtained. Making use of the expression of the flux in the continuity equation

$$\begin{aligned}
&\frac{\partial \rho}{\partial t} + \nabla \cdot (\rho \bar{v}) = 0 \ \text{ Overall continuity equation} \\
&c\frac{Dx_\alpha}{Dt} = -\nabla \cdot \bar{J}_\alpha + (R_\alpha - x_\alpha \sum_\beta^N R_\beta) \\
&\rho \frac{D\bar{v}}{Dt} = -\nabla p + \mu \nabla^2 \bar{v} + \rho \bar{g} \ \text{ Momentum} \\
&\rho \hat{c}_p \frac{DT}{Dt} = -\nabla \cdot \bar{q} - \left(\frac{\partial \ln \rho}{\partial \ln T} \right)_p \frac{Dp}{Dt} - \boldsymbol{\tau} : \nabla \bar{v} \ \text{ Energy}
\end{aligned} \tag{1.18}$$

All the latter equations needs to be solved simultaneously in order to obtain the T, p, ω distributions.
Considering the continuity equation for a species α in molar term

$$c\frac{Dx_\alpha}{Dt} = -\nabla \cdot \bar{J}_\alpha + (R_\alpha - x_\alpha \sum_\beta^N R_\beta) \tag{1.19}$$

For a steady state process, with fixed membrane and no reactions inside the membrane

$$\nabla \cdot \bar{J}_\alpha = 0 \tag{1.20}$$

Also, considering the mass transfer to happen only perpendicularly to the membrane

$$\frac{dJ_\alpha}{dz} = 0 \tag{1.21}$$

Considering the flux equations for porous and homogeneous membranes (1.14 and 1.17) and substituting them into the continuity equation

$$\begin{aligned}
&\frac{d}{dz}\left(cD_{\alpha,\beta} \frac{dx_\alpha}{dz} \right) = 0 \ \text{ Solution-Diffusion model} \\
&\frac{d}{dz}\left(cD_{\alpha,\beta} \frac{dp}{dz} \right) = 0 \ \text{ Pore-flow model}
\end{aligned} \tag{1.22}$$

In the framework of the solution-diffusion model the aim is to link the flux equation and the continuity equation to the conditions in the mixture bathing the membrane. It is therefore necessary to consider the conditions at the membrane interfaces: local equilibrium assumption between the mixture and the membrane surface on both sides of the membrane (permeate or retentate) has been made.

$$\begin{aligned} &\frac{d}{dz}\left(cD_{\alpha,\beta}\frac{dx_\alpha}{dz}\right)=0 \\ &z=0;\;\; x_\alpha = x^I_{\alpha,R} \\ &z=\delta;\;\; x_\alpha = x^I_{\alpha,P} \end{aligned} \tag{1.23}$$

General solution $x(z)$=$A_2 z$+A_1, where A_1, A_2 can be retrieved from the boundary conditions obtaining

$$J_\alpha = cD_{\alpha,\beta}\frac{x^I_{\alpha,R}-x^I_{\alpha,P}}{\delta} \tag{1.24}$$

where,

- $x^I_{\alpha,R}, c^I_{\alpha,R}, x^I_{\alpha,P}, c^I_{\alpha,P}$: molar fractions and compositions for component α within the membrane but either at the feed or permeate interface;
- δ: membrane thickness.

Determination of the species compositions at the membrane interfaces

$x^I_{\alpha,R}$ and $x^I_{\alpha,P}$ have to be expressed as a function of the conditions outside the membrane. The adopted procedure follows:

- local equilibrium at the membrane interface;
- obtaining $x^I_{\alpha,R}$ and $x^I_{\alpha,P}$ from isofugacity condition;
- substituting $x^I_{\alpha,R}$ and $x^I_{\alpha,P}$ into the flux equation.

The general form for liquid and gas fugacities in a liquid or gas mixture are:

Liquid fugacity

$$\begin{aligned} f^L_\alpha(T,p,\bar{x}) &= f^L_\alpha(T,p)x_\alpha\gamma_\alpha(T,p,\bar{x}) \\ &= \left[f^V_\alpha(T,p^*(T))\exp\int_{p^*}^{p}\frac{\tilde{v}_{\alpha,l}}{RT}dp\right]x_\alpha\gamma_\alpha \\ &= p^*(T)\left[\exp\int_0^{p^*}\frac{(z-1)}{p}dp\right]\left[\exp\int_{p^*}^{p}\frac{\tilde{v}_{\alpha,l}}{RT}dp\right]x_\alpha\gamma_\alpha \\ &= p^*_\alpha(T)\phi^V_\alpha(T,p^*_\alpha)\mathfrak{F}_\alpha x_\alpha\gamma_\alpha \end{aligned} \tag{1.25}$$

where,

- f^V_α is the pure vapor fugacity of component α;

- $\phi_\alpha^V = \exp \int_0^{p^*} \frac{(z-1)}{p} dp$ is the pure vapor fugacity coefficient of component α;
- $\mathfrak{F}_\alpha = \exp \int_{p^*}^{p} \frac{\tilde{v}_{\alpha,l}}{RT} dp$ is the Poyting factor and $\tilde{v}_{\alpha,l}$ the pure liquid molar volume of species α.

Gas fugacity

$$f_\alpha^V(T, p, \bar{y}) = p y_\alpha \phi_\alpha(T, p, \bar{x}) \tag{1.26}$$

where,

- y_α is the vapor molar composition of species α;
- ϕ_α is the mixture vapor fugacity coefficient of component α.

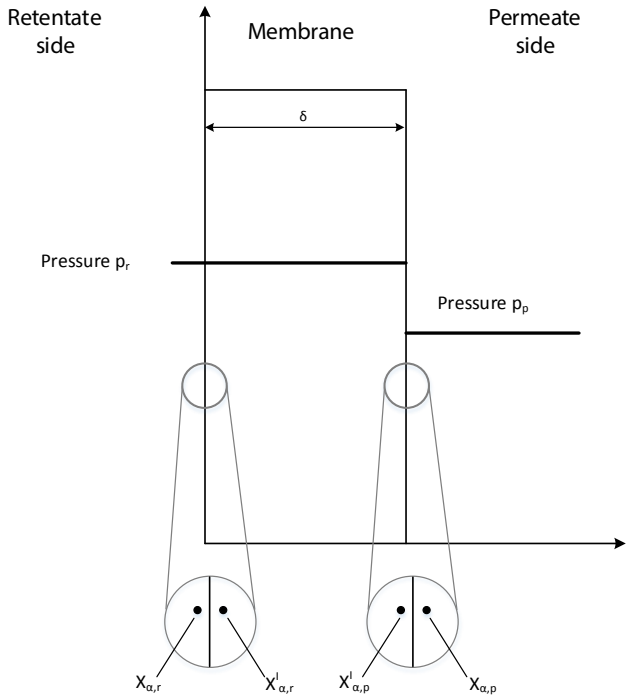

Figure 1.6: Identification of the interface membrane and bulk sides compositions

1.5 Reverse Osmosis

Reverse osmosis and normal osmosis (dialysis) are directly related processes.
In simple terms, if a permselective membrane (i e. a membrane freely permeable to water, but much less permeable to salt) is used to separate a salt solution from pure water, water will pass through the membrane from the pure-water side of the membrane into the side less concentrated in water (salt side). This process is called normal osmosis. If a hydrostatic pressure is applied to the salt side of the membrane, the flow of water can be retarded and, when the applied pressure is sufficient, the flow ceases.
The hydrostatic pressure required to stop the water flow is called the osmotic pressure ($\Delta\pi$). If pressure greater than the osmotic pressure are applied to the salt side of the membrane, then the flow of water is reversed, and water begins to glow from the salt solution to the pure water side of the membrane. This process is called reverse osmosis and is an important method of producing pure water from salt solutions.
In reverse osmosis, following the general procedure, the chemical potentials at both sides of the membrane are first equated. At the retentate interface, the pressure in the retentate solution and within the membrane are identical (see fig. 1.9c).

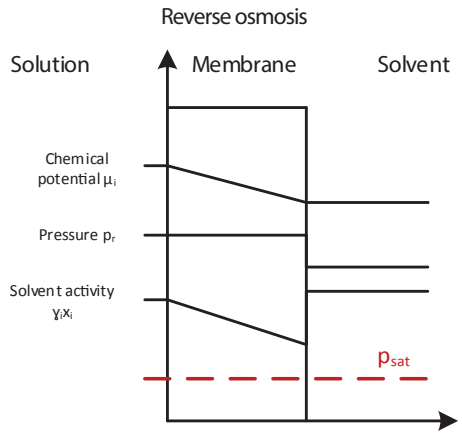

Figure 1.7: Pressure and concentration profiles in a reverse osmosis process.

Chemical Potentials At The Membrane Retentate Side Interface

Equating the fugacities at the retentate side interface of the membrane gives

$$f_{\alpha,r} = f^I_{\alpha,r} \tag{1.27}$$

and recalling (eq. 1.25)

$$\begin{aligned} \cancel{\left[f^V_\alpha \exp \int_{p^*}^{p_r} \frac{\tilde{v}_{\alpha,l}}{RT} dp \right]} x_{\alpha,r}\gamma_\alpha(T, p_r, x_{\alpha,r}) = \\ = \cancel{\left[f^V_\alpha \exp \int_{p^*}^{p_r} \frac{\tilde{v}_{\alpha,l}}{RT} dp \right]} x^I_{\alpha,r}\gamma_\alpha(T, p_r, x^I_{\alpha,r}) \end{aligned} \tag{1.28}$$

which leads to

$$x_{\alpha,r}\gamma_{\alpha,r} = x^I_{\alpha,r}\gamma^I_{\alpha,r} \tag{1.29}$$

Chemical Potentials At The Membrane Permeate Side Interface

At the permeate side interface, a pressure difference exists (as shown in fig. 1.9 (c)) from p_r within the membrane to p_p in the permeate solution. Equating the fugacities across this interface gives

$$f_{\alpha,p} = f^I_{\alpha,p} \tag{1.30}$$

Substituting the appropriate expression for the fugacity of a liquid in a mixture (eq. 1.25) yields

$$\begin{aligned} \left[\cancel{f^V_\alpha} \exp \int_{p^*}^{p_p} \frac{\tilde{v}_{\alpha,l}}{RT} dp \right] x_{\alpha,p}\gamma_{\alpha,p}(T, p_p, x_{\alpha,p}) = \\ = \left[\cancel{f^V_\alpha} \exp \int_{p^*}^{p_r} \frac{\tilde{v}_{\alpha,l}}{RT} dp \right] x^I_{\alpha,p}\gamma_{\alpha,p}(T, p_r, x^I_{\alpha,p}) \end{aligned} \tag{1.31}$$

which leads to

$$x_{\alpha,p}\gamma_{\alpha,p} = x^I_{\alpha,p}\gamma^I_\alpha \exp \int_{p_p}^{p_r} \frac{\tilde{v}_{\alpha,l}}{RT} dp \tag{1.32}$$

Rearranging eq. 1.29 and 1.32

$$\begin{aligned} x^I_{\alpha,r} &= x_{\alpha,r} \frac{\gamma_{\alpha,r}}{\gamma^I_{\alpha,r}} \\ x^I_{\alpha,p} &= x_{\alpha,p} \frac{\gamma_{\alpha,p}}{\gamma^I_{\alpha,p}} \left\{ \exp \left[-\frac{\tilde{v}_{\alpha,l}}{RT}(p_r - p_p) \right] \right\} \end{aligned} \tag{1.33}$$

Substituting these two terms into the continuity equation (flux)

$$\begin{aligned} J_\alpha &= cD_{\alpha,\beta}\frac{x^I_{\alpha,R} - x^I_{\alpha,P}}{\delta} = \\ &= \frac{cD_{\alpha,\beta}}{\delta}\left\{x_{\alpha,r}\frac{\gamma_{\alpha,r}}{\gamma^I_{\alpha,r}} - x_{\alpha,p}\frac{\gamma_{\alpha,p}}{\gamma^I_{\alpha,p}}\exp\left[-\frac{\tilde{v}_{\alpha,l}}{RT}(p_r - p_p)\right]\right\} \end{aligned} \tag{1.34}$$

which can be simplified assuming that the ratio between the activity coefficient is the same at the retentate or at the permeate side:

$$J_\alpha \approx \frac{cD_{\alpha,\beta}}{\delta}\frac{\gamma_{\alpha,r}}{\gamma^I_{\alpha,r}}\left\{x_{\alpha,r} - x_{\alpha,p}\exp\left[-\frac{\tilde{v}_{\alpha,l}}{RT}(p_r - p_p)\right]\right\} \tag{1.35}$$

The latter equation can be further rearranged

$$\begin{aligned} J_\alpha &= \frac{K^L_\alpha D_{\alpha,\beta}}{\delta}\left\{x_{\alpha,r} - x_{\alpha,p}\exp\left[-\frac{\tilde{v}_{\alpha,l}}{RT}(p_r - p_p)\right]\right\} = \\ &= \frac{Q_\alpha}{\delta}\left\{x_{\alpha,r} - x_{\alpha,p}\exp\left[-\frac{\tilde{v}_{\alpha,l}}{RT}(p_r - p_p)\right]\right\} \end{aligned} \tag{1.36}$$

where

- the product $c\frac{\gamma_{\alpha,r}}{\gamma_{\alpha,r}}^I = K^L_\alpha$ is defined as the sorption coefficient of species α in the membrane matrix;
- the product $D_{\alpha,\beta}\frac{\gamma_{\alpha,r}}{\gamma^I_{\alpha,r}} = Q_\alpha$ is often referred to the permeability of species α in the membrane. It represents the extent if which a species dissolves and diffuses through a membrane. Permeability is also the parameter which is usually experimentally measured.

Often, the flux equation for liquid is reported in term of concentrations of species α in a liquid mixture

$$J_\alpha = \frac{Q^*_\alpha}{\delta}\left\{c_{\alpha,r} - c_{\alpha,p}\exp\left[-\frac{\tilde{v}_{\alpha,l}}{RT}(p_r - p_p)\right]\right\} \tag{1.37}$$

where,

- Q^*_α in now accounting for the change from molar fraction to concentration.

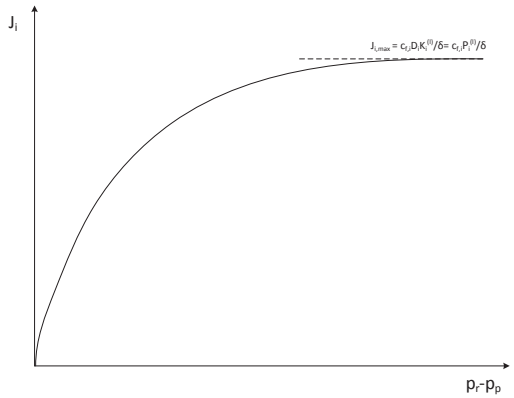

Figure 1.8: Flux of component i as a function of $\Delta p = p_r - p_p$.

Some insights can be gained by plotting the flux equation as a function of the $\Delta p = (p_r - p_p)$ in fig. 1.8. Very large pressure differences across the membrane produce relatively small concentration gradients and therefore an flux increase.

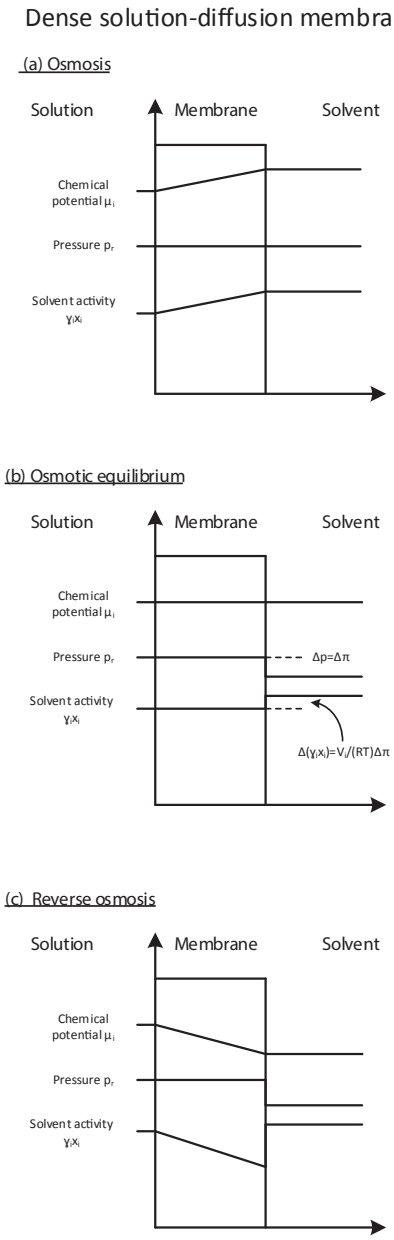

Figure 1.9: Chemical potential, pressure, and solvent activity profiles in an osmotic membrane according to the solution-diffusion model.

1.5.1 An Application: Water Desalination

Reverse osmosis is mostly used for desalting water. Membranes that are permeable to water, but essentially impermeable to salt are exploited. The objective of water desalination is the production of fresh water at the permeate side. Figure 1.10 displays the schematic of a membrane module for water desalination. A pressure difference is applied across the membrane, which sees a liquid mixture at both sides. Pressurized water containing dissolved salts contacts the feed side of the membrane, while water depleted of salt is withdrawn as low-pressure permeate. This section aims at expressing the flux equations in terms of the pressure gradient through the membrane and linearize them.

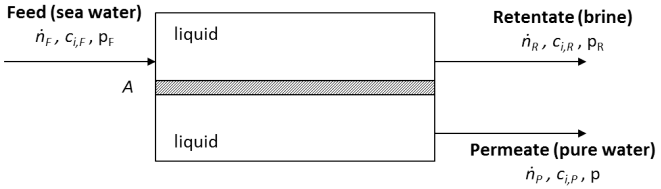

Figure 1.10: Schematic of a membrane module for reverse osmosis

The equation of the flux for reverse osmosis, assuming the ratio of activity coefficients equal at retentate and permeate side, is here reported for convenience:

$$J_\alpha = \frac{cD_{\alpha,\beta}}{\delta}\frac{\gamma_{\alpha,r}}{\gamma^I_{\alpha,r}}\left\{x_{\alpha,r} - x_{\alpha,p}\exp\left[-\frac{\tilde{v}_{\alpha,l}}{RT}(p_r - p_p)\right]\right\} \tag{1.38}$$

Where the subscripts r and p indicate the retentate and permeate conditions, respectively.This equation is often reported in terms of concentration, either mass or molar based:

$$x_\alpha = \frac{c_\alpha}{c_{tot}} \rightarrow x_{\alpha,f} = \frac{c_{\alpha,f}}{c_{tot,f}}; x_{\alpha,p} = \frac{c_{\alpha,p}}{c_{tot,p}} \tag{1.39}$$

Therefore,

$$J_\alpha = \frac{cD_{\alpha,\beta}}{\delta}\frac{\gamma_{\alpha,r}}{\gamma^I_{\alpha,r}}\left\{\frac{c_{\alpha,r}}{c_{tot,r}} - \frac{c_{\alpha,p}}{c_{tot,p}}\exp\left[-\frac{\tilde{v}_{\alpha,l}}{RT}(p_r - p_p)\right]\right\} \tag{1.40}$$

If $c_{tot,r} \cong c_{tot,p} = c_{tot}$ it is obtained:

$$\begin{aligned} J_\alpha &= \frac{D_{\alpha,\beta}}{\delta}\underbrace{\frac{\gamma_{\alpha,r}}{\gamma^I_{\alpha,r}}x^I_\alpha}_{K_\alpha}\left\{c_{\alpha,r} - c_{\alpha,p}\exp\left[-\frac{\tilde{v}_{\alpha,l}}{RT}(p_r - p_p)\right]\right\} \\ &= \frac{\mathfrak{P}_\alpha}{\delta}\left\{c_{\alpha,r} - c_{\alpha,p}\exp\left[-\frac{\tilde{v}_{\alpha,l}}{RT}(p_r - p_p)\right]\right\} \end{aligned} \tag{1.41}$$

From an operation point of view, water desalination is driven by the pressure difference at membrane sides. In the following, the required pressure difference for different operation conditions is investigated.
The equilibrium condition defines the osmotic pressure, $\Delta\pi$. It essentially represents the minimum partial pressure difference necessary for the reverse osmosis to occur. At equilibrium, the water flux is null, $J_w = 0$, locally, at any position along the membrane. It follows that

$$J_w = 0 = \frac{Q_w}{\delta} \left\{ x_{w,r}(z) - x_{w,p}(z) \ \exp\left[-\frac{\tilde{v}_w}{R\,T} \underbrace{(p_r - p_p)}_{\Delta\pi} \right] \right\} \tag{1.42}$$

Therefore,

$$\Delta\pi = -\frac{R\,T}{\tilde{v}_w} \ \ln\frac{x_{w,r}(z)}{x_{w,p}(z)} = \frac{R\,T}{\tilde{v}_w} \ \ln\frac{x_{w,p}(z)}{x_{w,r}(z)} \tag{1.43}$$

Assuming $x_{w,p}(z) = 1, \forall z$

$$\Delta\pi = \frac{R\,T}{\tilde{v}_w} \ \ln\frac{1}{x_{w,r}(z)} \tag{1.44}$$

Equation 1.44 states that the higher $x_{w,r}(z)$, the lower the osmotic pressure.
Three scenarios can be identified referring to equation 1.41:

- $p_r - p < \Delta\pi \implies \exp[\cdot] > 1$. Normal osmosis takes place. The water flows from the pure-water side to the sea-water side.
- $p_r - p = \Delta\pi \implies \exp[\cdot] = 1$. Osmotic equilibrium is reached. No flux occurs, since the osmotic pressure is counterbalance by the pressure difference.
- $p_r - p > \Delta\pi \implies \exp[\cdot] < 1$. Reverse osmosis takes place. The water flows from the sea-water side to the pure-water side.

Such a conclusion can be reached by mean of the balance equations around the membrane module. In particular:

- *Overall material balance*

$$\dot{n}_f = \dot{n}_p + \dot{n}_r \tag{1.45}$$

- *Water material balance*

$$\dot{n}_f \ x_{w,f} = \dot{n}_p \ x_{w,p} + \dot{n}_r \ x_{w,r} \tag{1.46}$$

- *Flux equation*

$$J_w = \frac{Q_w}{\delta} \left\{ x_{w,r}(z) - x_{w,p}(z) \ \exp\left[-\frac{\tilde{v}_w}{R\,T}(p_f - p_p) \right] \right\} \tag{1.47}$$

- *Composition equation*

$$\sum_i x_i = 1, \forall i \tag{1.48}$$

Where i represents the generic component in the feed flow.
In the following, two different cases are analysed based on different flow conditions at membrane sides.

Case A. The following assumptions are made: (I) The water fraction in the retentate is constant, equal to the feed water fraction; (II) The water fraction at permeate side is constant, independent of membrane position; (III) The pressure is also constant at both sides of the membrane. As a consequence,

$$\begin{cases} x_{w,r}(z) = x_{w,f} \ \ \forall z \\ x_{w,p}(z) = x_{w,p} \ \ \forall z \end{cases} \tag{1.49}$$

Recalling the definition of osmotic pressure, the flux equations can be re-written as a function of the osmotic pressure and pressure difference:

$$x_{w,p} = x_{w,f} \exp\left(\frac{\tilde{v}_w}{R\,T}\,\Delta\pi\right) \tag{1.50}$$

Thus,

$$J_w = \frac{Q_w}{\delta}\,x_{w,f}\,\left\{1 - \exp\left[-\frac{\tilde{v}_w}{R\,T}\,\left(p_f - p_p - \Delta\pi\right)\right]\right\} \tag{1.51}$$

For the conditions holding in most of real water desalination applications, the aforementioned flux equation can be linearized. In particular, noting the small specific volume for liquid mixtures, $v_w \longrightarrow 0$, and recalling the Taylor-Maclaurin series for the exponential function

$$\begin{aligned} e^{-x} &= 1 - x + \frac{x^2}{2!} - \frac{x^3}{3!} + ... \ \forall x \\ \lim_{x\to 0} e^{-x} &= 1 - x \end{aligned} \tag{1.52}$$

it is possible to write,

$$\begin{aligned} J_w &= \frac{Q_w}{\delta}\,x_{w,f}\,\left\{\frac{\tilde{v}_w}{R\,T}\,\left[(p_f - p_p) - \Delta\pi\right]\right\} \\ J_w &= \frac{Q_w}{\delta}\,x_{w,f}\,\frac{\tilde{v}_w}{R\,T}\,\left[(p_f - p_p) - \Delta\pi\right] \end{aligned} \tag{1.53}$$

Therefore,

- $p_r - p < \Delta\pi \implies J_w < 0$. Normal osmosis takes place. The water flows from the pure-water side to the sea-water side.

- $p_r - p = \Delta\pi \implies J_w = 0$. Osmotic equilibrium is reached. No flux occurs, since the osmotic pressure is counterbalance by the pressure difference.
- $p_r - p > \Delta\pi \implies J_w > 0$. Reverse osmosis takes place. The water flows from the sea-water side to the pure-water side.

The linearization above is reliable for highly selective membranes, $x_{w,p} \approx 1$, and small water recovery, $x_{w,r}(z) \approx x_{w,f}\ \forall z$. In fact, different assumptions can lead to a slight deviation from linearity. As an example, the perfect mixing condition is investigated below.

Case B. Perfect mixing conditions are assumed. This implies: (I) Constant molar fraction at retentate side, but different than in the feed stream; (II) Constant molar fraction at permeate side; (III) Constant pressures at both membrane sides. As a consequence,

$$\begin{cases} x_{w,r}(z) = x_{w,r}\ \forall z,\ \neq x_{w,f} \\ x_{w,p}(z) = x_{w,p}\ \forall z \end{cases} \tag{1.54}$$

In this framework the equation system becomes

$$\begin{cases} \Delta\pi = \frac{R\ T}{\tilde{v}_w} ln \frac{x_{w,p}(z)}{x_{w,r}(z)} = \frac{R\ T}{\tilde{v}_w} ln \frac{x_{w,p}}{x_{w,r}} \\ \dot{n}_r = \dot{n}_f - \dot{n}_p = \dot{n}_f(1-\theta) \\ x_{w,r} = \frac{\dot{n}_f\ x_{w,f} - \dot{n}_p\ x_{w,p}}{\dot{n}_r} = \frac{x_{w,f} - \theta\ x_{w,p}}{1-\theta} \underbrace{\approx \frac{x_{w,f} - \theta}{1-\theta}}_{\text{for } x_{w,p} \approx 1} \\ J_w = \frac{Q_w}{\delta}\ x_{w,r}\ \left\{1 - \exp\left[-\frac{\tilde{v}_w}{R\ T}\ (p_f - p_p - \Delta\pi)\right]\right\} \end{cases} \tag{1.55}$$

It is worth noticing how an increase in the stage cut, θ, brings to: (I) A decrease in $x_{w,r}$; (II) An increase in osmotic pressure $\Delta\pi$; (III) An decrease in flux J_w for constant pressure difference. The water flux can be determined by solving the system above. Figure 1.11 reports the water flux as a function of the pressure difference for the ideal case (i.e. $x_{w,r} = x_{w,f}$, equivalent to $c_{w,r} = c_{w,f}$) and for the perfect mixing case. A lower water flux and a slight deviation from linearity is registered in the perfect mixing case.

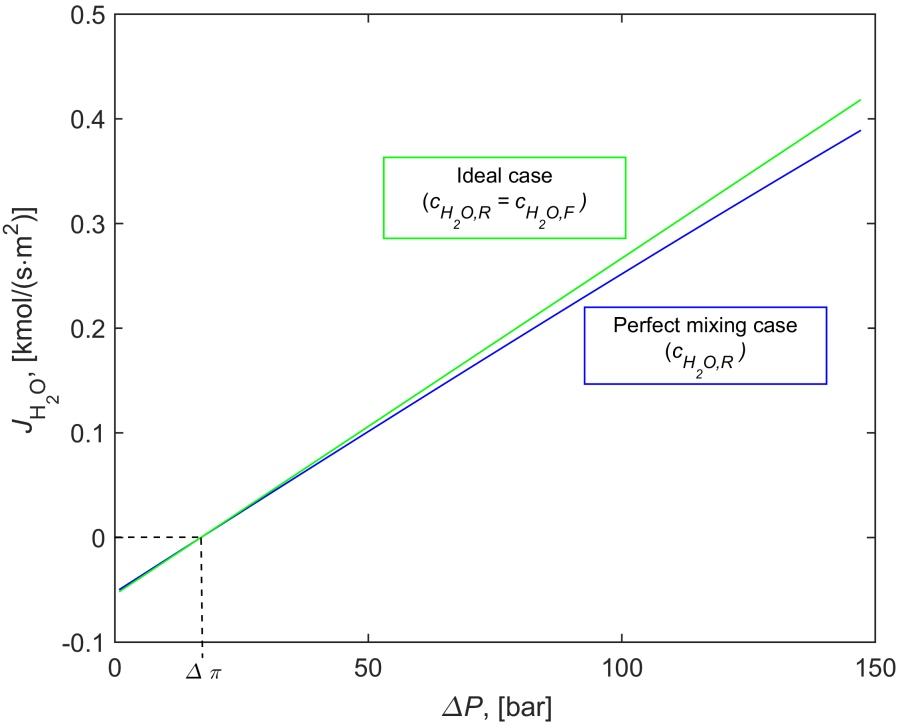

Figure 1.11: Ideal and perfect mixing relationship between the water flux and the pressure difference in a reverse osmosis application.

1.6 Gas Separation

Membranes modules can be also used to perform gases separations. A mathematical expression for the flux a gaseous component through the membrane is therefore needed. The typical process conditions for a gas separation process are shown in fig. 1.12 where a high pressure gas mixture at p_r is fed to the feed side of the membrane while the permeate is removed at a lower pressure p_p at the downstream side. The pressure profile within the membrane is assumed constant and equal to p_r while the chemical potential gradient is due to the component partial pressure difference between feed and permeate concentrations.

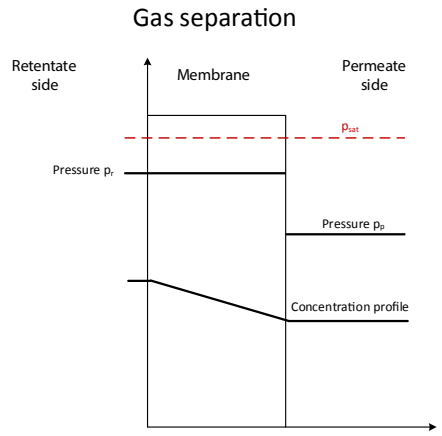

Figure 1.12: Pressure and concentration profiles in a gas separation process.

Chemical Potentials At The Membrane Retentate Side Interface

Equating the fugacities at the retentate side (feed) interface of the membrane gives

$$f_{\alpha,r} = f^I_{\alpha,r} \tag{1.56}$$

The assumption that once the gas is adsorbed in the membrane matrix it behaves as a liquid rather than a gas allows to write the fugacity of a component within the membrane as the fugacity of a species in a liquid mixture. Recalling (eq. 1.25)

$$\begin{aligned} y_{\alpha,r} p_r \phi_\alpha(T, p_r, y_{\alpha,r}) = \\ = \left[f^V_\alpha \exp \int_{p^*_\alpha}^{p_r} \frac{\tilde{v}_{\alpha,l}}{RT} dp \right] x^I_{\alpha,r} \gamma_\alpha(T, p_r, x^I_{\alpha,r}) \end{aligned} \tag{1.57}$$

which leads to, considering the $\phi_\alpha^V = 1$ and rearranging the latter equation

$$y_{\alpha,r} p_r \frac{\phi_\alpha(T, p_r, y_{\alpha,r})}{p_\alpha^*(T)\gamma_\alpha(T, p_r, x_{\alpha,r}^I)} = x_{\alpha,r}^I \exp\left[(p_r - p_\alpha^*)\frac{\tilde{v}_{\alpha,l}}{RT}\right] \tag{1.58}$$

the molar fraction, $y_{\alpha,r}^I$, therefore is

$$\begin{aligned} x_{\alpha,r}^I &= y_{\alpha,r} p_r \frac{\phi_\alpha(T, p_r, y_{\alpha,r})}{p_\alpha^*(T)\gamma_\alpha(T, p_r, x_{\alpha,r}^I)} \exp\left[-(p_r - p_\alpha^*)\frac{\tilde{v}_{\alpha,l}}{RT}\right] \\ &= K_\alpha^{G,r} p_{\alpha,r} \exp\left[-(p_r - p_\alpha^*)\frac{\tilde{v}_{\alpha,l}}{RT}\right] \end{aligned} \tag{1.59}$$

Chemical Potentials At The Membrane Permeate Side Interface

At the permeate side interface, a pressure difference exists from p_r within the membrane to p_p in the permeate gas stream. Equating the fugacities across this interface gives

$$f_{\alpha,p} = f_{\alpha,p}^I \tag{1.60}$$

Substituting the appropriate expression for the fugacity of a liquid in a mixture (eq. 1.25) yields

$$\begin{aligned} &y_{\alpha,p} p_p \phi_\alpha(T, p_p, y_{\alpha,p}) = \\ &\qquad = \left[f_\alpha^V \exp \int_{p_\alpha^*}^{p_r} \frac{\tilde{v}_{\alpha,l}}{RT} dp\right] x_{\alpha,p}^I \gamma_\alpha(T, p_r, x_{\alpha,p}^I) \end{aligned} \tag{1.61}$$

which leads to the molar fraction of species α at the membrane interface

$$\begin{aligned} x_{\alpha,p}^I &= y_{\alpha,p} p_p \frac{\phi_\alpha(T, p_p, y_{\alpha,p})}{p_\alpha^*(T)\gamma_\alpha(T, p_p, x_{\alpha,p}^I)} \exp\left[-(p_r - p_\alpha^*)\frac{\tilde{v}_{\alpha,l}}{RT}\right] \\ &= K_\alpha^{G,p} p_{\alpha,p} \exp\left[-(p_r - p_\alpha^*)\frac{\tilde{v}_{\alpha,l}}{RT}\right] \end{aligned} \tag{1.62}$$

Substituting equations 1.59 and 1.62 into the flux equation for binary mixtures

$$\begin{aligned} J_\alpha = \frac{cD_{\alpha,\beta}}{\delta}\Bigg\{ &K_\alpha^{G,r} p_{\alpha,r} \exp\left[-(p_r - p_\alpha^*)\frac{\tilde{v}_{\alpha,l}}{RT}\right] + \\ &- K_\alpha^{G,p} p_{\alpha,p} \exp\left[-(p_r - p_\alpha^*)\frac{\tilde{v}_{\alpha,l}}{RT}\right]\Bigg\} \end{aligned} \tag{1.63}$$

which can be simplified assuming the equality between the sorption coefficients respectively on the retentate (feed) and permeate side:

$$\begin{aligned} J_\alpha &= c\frac{D_{\alpha,\beta}K_\alpha^G}{\delta}\left(p_{\alpha,r}-p_{\alpha,p}\right)\exp\left[-(p_r-p_\alpha^*)\frac{\tilde{v}_{\alpha,l}}{RT}\right]= \\ &= c\frac{D_{\alpha,\beta}K_\alpha^G}{\delta}\left(p_{\alpha,r}-p_{\alpha,p}\right)\mathfrak{F}_\alpha \end{aligned} \tag{1.64}$$

Considering the fact that the Poynting correction factor $\mathfrak{F}_\alpha$ is close to 1 for system at relatively low pressure

$$J_\alpha = \frac{D_{\alpha,\beta}K_{G,\alpha}^*}{\delta}\left(p_{\alpha,r}-p_{\alpha,p}\right) = \frac{Q_\alpha}{\delta}\left(p_{\alpha,r}-p_{\alpha,p}\right) \tag{1.65}$$

The flux of gas species α across a membrane is indipendent from the total pressure while depends on the difference in partial pressures across the membrane.

1.7 Pervaporation

Pervaporation can be considered as an intermediate separation process between gas separation and reverse osmosis processes. The peculiarity of the pervaporation process is that the permeate pressure is fixed to a value below the saturation pressure of the permeating mixture therefore the stream condition is a vapor. The physical state of the feed stream is a liquid due to the fact that the operating pressure is above the vapor pressure of the mixture at the operative temperature. The system is represented in fig. 1.13.

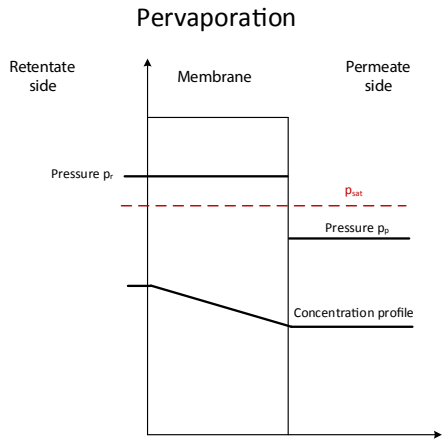

Figure 1.13: Pressure and concentration profiles in a pervaporation process.

Feed conditions
Retentate membrane interface in contact with a feed fluid which is liquid at $p > p^{sat}$.

Permeate conditions
Permeate membrane interface in contact with a permeate fluid which is vapor at $p < p^{sat}$.
During a pervaporation process the liquid stream that is permeating through the membrane undergoes vaporization. In a general approach an energy balance should be coupled with material balances in order to account for either mass and heat transfer effects. For sake of simplicity the isofugacity conditions, imposed at the membrane interfaces, are applied to an isothermal pervaporation membrane where the change in temperature effect is not occurring.

Chemical Potentials At The Membrane Retentate Side Interface

Equating the fugacities at the retentate side interface of the membrane gives

$$f_{\alpha,r} = f^I_{\alpha,r} \tag{1.66}$$

and recalling (eq. 1.25)

$$\begin{aligned} \cancel{\left[f^V_\alpha \exp \int_{p^*}^{p_r} \frac{\tilde{v}_{\alpha,l}}{RT} dp \right]} x_{\alpha,r}\gamma_\alpha(T, p_r, x_{\alpha,r}) = \\ = \cancel{\left[f^V_\alpha \exp \int_{p^*}^{p_r} \frac{\tilde{v}_{\alpha,l}}{RT} dp \right]} x^I_{\alpha,r}\gamma_\alpha(T, p_r, x^I_{\alpha,r}) \end{aligned} \tag{1.67}$$

which leads to

$$x_{\alpha,r}\gamma_{\alpha,r} = x^I_{\alpha,r}\gamma^I_{\alpha,r} \tag{1.68}$$

Rearranging the latter equation:

$$x^I_{\alpha,r} = x_{\alpha,r}\frac{\gamma_{\alpha,r}}{\gamma^I_{\alpha,r}} \tag{1.69}$$

Chemical Potentials At The Membrane Permeate Side Interface

At the permeate side interface, a pressure difference exists from p_r within the membrane to p_p in the permeate gas stream. Equating the fugacities across this interface gives

$$f_{\alpha,p} = f^I_{\alpha,p} \tag{1.70}$$

The expressions for the fugacity of a liquid (eq. 1.25) at the membrane interface and for the fugacity of a vapor (eq. 1.26) at the permeate interface (bulk side) leads to

$$\begin{aligned} y_{\alpha,p}p_p\phi_\alpha(T, p_p, y_{\alpha,p}) = \\ = \left[f^V_\alpha \exp \int_{p^*_\alpha}^{p_r} \frac{\tilde{v}_{\alpha,l}}{RT} dp \right] x^I_{\alpha,p}\gamma_\alpha(T, p_r, x^I_{\alpha,p}) \end{aligned} \tag{1.71}$$

considering the $\phi^V_\alpha = 1$ and rearranging the latter equation for expressing the molar fraction of species α at the membrane interface

$$x^I_{\alpha,p} = y_{\alpha,p}p_p \frac{\phi_\alpha(T, p_r, y_{\alpha,p})}{p^*_\alpha(T)\gamma_\alpha(T, p_p, x^I_{\alpha,p})} \exp\left[-(p_r - p^*_\alpha)\frac{\tilde{v}_{\alpha,l}}{RT} \right] \tag{1.72}$$

Substituting equations 1.69 and 1.72 into the flux equation for binary mixtures

$$J_\alpha = \frac{cD_{\alpha,\beta}}{\delta}\Bigg\{ x_{\alpha,r} \underbrace{\frac{\gamma_{\alpha,r}}{\gamma^I_{\alpha,r}}}_{K^*_{L,\alpha}} + - y_{\alpha,p}p_p \underbrace{\frac{\phi_\alpha(T,p_r,y_{\alpha,p})}{p^*_\alpha(T)\gamma_\alpha(T,p_p,x^I_{\alpha,p})}}_{K^*_{V,\alpha}} \underbrace{\exp\left[-(p_r-p^*_\alpha)\frac{\tilde{v}_{\alpha,l}}{RT}\right]}_{\approx 1} \Bigg\} \tag{1.73}$$

Considering the fact that the Poynting correction factor $\mathfrak{F}_\alpha$ is close to 1 for system at relatively low pressure and introducing the sorption coefficients in the latter equation:

$$J_\alpha = \frac{D_{\alpha,\beta}}{\delta}\left[x_{\alpha,r}K^*_{L,\alpha} - y_{\alpha,p}p_pK^*_{V,\alpha}\right] \tag{1.74}$$

Equation 1.74 can be written as

$$J_\alpha = \frac{D_{\alpha,\beta}K^*_{V,\alpha}}{\delta}\left[x_{\alpha,r}H_{L,\alpha} - y_{\alpha,p}p_p\right] = \frac{Q^V_{\alpha,\beta}}{\delta}\left[x_{\alpha,r}H_{L,\alpha} - y_{\alpha,p}p_p\right] \tag{1.75}$$

where,

- $H_{L,\alpha} = \frac{K^*_{L,\alpha}}{K^*_{V,\alpha}}$ represents the Henry constant solubility for component α ;
- $Q^V_{\alpha,\beta}$ represents the vapor permeability of component α in the pervaporation membrane.

1.8 Unified View Of The Solution Diffusion Model

The solution-diffusion model is used to calculate the concentration gradients established among a membrane layer in reverse osmosis, gas separation and pervaporation processes.

Reverse osmosis

$$J_\alpha = \frac{Q_\alpha}{\delta}\left\{x_{\alpha,r} - x_{\alpha,p}\exp\left[-\frac{\tilde{v}_{\alpha,l}}{RT}(p_r - p_p)\right]\right\}$$

$$J_\alpha = \frac{Q^*_\alpha}{\delta}\left\{c_{\alpha,r} - c_{\alpha,p}\exp\left[-\frac{\tilde{v}_{\alpha,l}}{RT}(p_r - p_p)\right]\right\}$$

Gas permeation

$$J_\alpha = \frac{Q_\alpha}{\delta}\left(p_{\alpha,r} - p_{\alpha,p}\right)\exp\left[-(p_r - p^*_\alpha)\frac{\tilde{v}_{\alpha,l}}{RT}\right]$$

Pervaporation

$$J_\alpha = \frac{cD_{\alpha,\beta}}{\delta}\left\{x_{\alpha,r}K^*_{L,\alpha} - y_{\alpha,p}p_pK^*_{V,\alpha}\exp\left[-(p_r - p^*_\alpha)\frac{\tilde{v}_{\alpha,l}}{RT}\right]\right\}$$

Fig. 1.14 summarizes the typical reverse osmosis, gas separation and pervaporation processes pressure profiles. By considering the permeate mixture saturation pressure p_{sat} as a reference pressure it can be stated that for the case of reverse osmosis both retentate and permeate streams are subcooled liquids. When the permeate operating pressure is set below the permeate mixture vapor pressure the retentate will be a liquid while the permeate will be a vapor (pervaporation case). In the case of gas separations both retentate and permeate streams are below the mixtures saturation pressures, this is indeed the case of two stable gas mixtures respectively in the feed and permeate sides.

All the processes can be represented in a single diagram as shown in fig. 1.15 where the performance of each process, at any retentate and permeate pressures condition, can be indicated as a point within the figure.
The flux of component α can be normalized using $J_{\alpha,max}$ and expressed as a function of the ratio between the operative retentate operative pressure versus the retentate saturation pressure. A value of the ratio below one defines the retentate mixture as a vapor while the value of one signifies the transition between vapor to liquid state for the retentate. By varying the permeate pressure from values below its vapor pressure to values for which the permeate aggregation state is liquid ($p_p > p_{p,\text{sat}}$) different membrane separation processes can be identified. The liming flux corresponds to the permeation rate of a retentate liquid which is not a function of the applied Δp anymore.

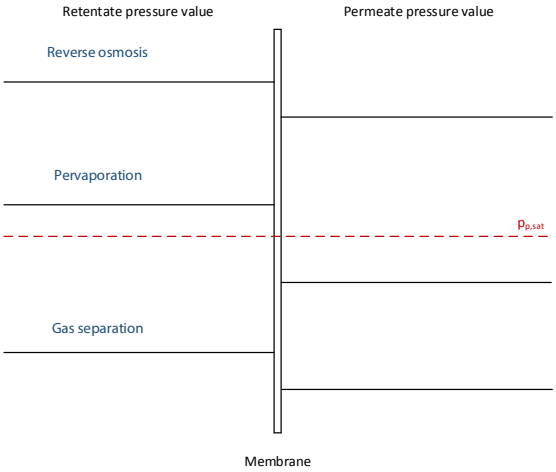

Figure 1.14: Pressure profiles for different membrane separation processes: gas separation, pervaporation and reverse osmosis.

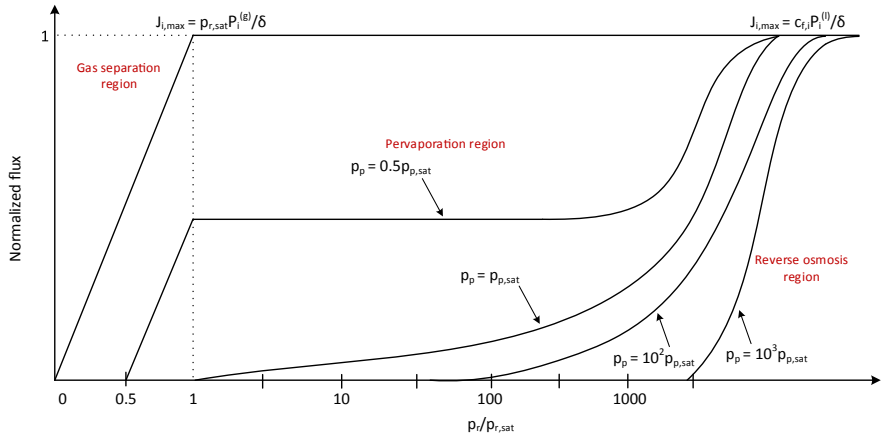

Figure 1.15: Normalized flux profiles for different membrane separation processes: gas separation, pervaporation and reverse osmosis.

REFERENCES

1. J. G. Wijmans, R. W. Baker, *The solution-diffusion model: a review*, Journal of Membrane Science **1995** 1-21.
2. Bird, R.B., Stewart, W.E. and Lightfoot, E.N., *Transport Phenomena*, John Wiley & Sons **1995** (First Edition).

CHAPTER 2

FROM IDEAL TO REAL: LOSSES MECHANISMS IN MEMBRANES

In membrane separation processes, a gas or a liquid mixture contacts the feed side of the membrane, and a permeate enriched in one of the components of the mixture is withdrawn from the downstream side of the membrane. Because feed mixture components permeate at different rates, concentration gradients can form in the fluids on both sides of the membrane. In this case, the concentration at the membrane surfaces are not the same as the bulk fluid concentrations. This phenomenon is called concentration polarization and it affects the overall mass flux through the membrane as shown in fig. 2.1. Eq. 1.36 provides a theoretical explanation of the flux behaves under a superimposed pressure gradient but as shown in fig. 2.1 the real flux values are less that the theoretical ones, in and show a non-linear behavior with increasing the applied gradient pressure.

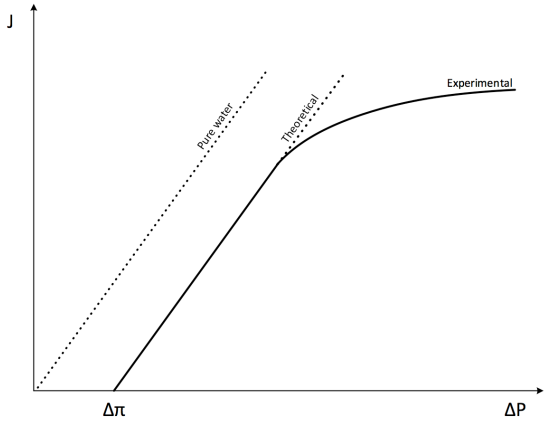

Figure 2.1: Membrane flux over applied gradient pressure.

Membrane modules achievable performances not only depend on membranes characteristics but also on the solution fluid-dynamics which strongly affects the mass transport rate from the bulk liquid phase to the membrane.
In a membrane module the different components are transported towards the membrane because of the overall convective motion of the mixture. Due to the membrane rejection (not every component is able to permeate through the membrane) toward a specific permeant a polarization concentration of this component is likely to occur in the mass transfer layer close to the membrane. This implies that, at the retentate membrane interface, the concentration of the component which is rejected assumes higher values with respect to the bulk concentration. The physical consequence of this is that a diffusive flux of the not permeable component is established in the opposite direction of the convective flux (from the membrane interface to the bulk liquid phase). The importance of concentration polarization depends on the membrane separation process. Concentration polarization can significantly affect membrane performance in reverse osmosis, but it is usually well controlled in industrial systems. On the other hand, membrane performance in ultrafiltration, electrodialysis, and some pervaporation processes is seriously affected by concentration polarization.

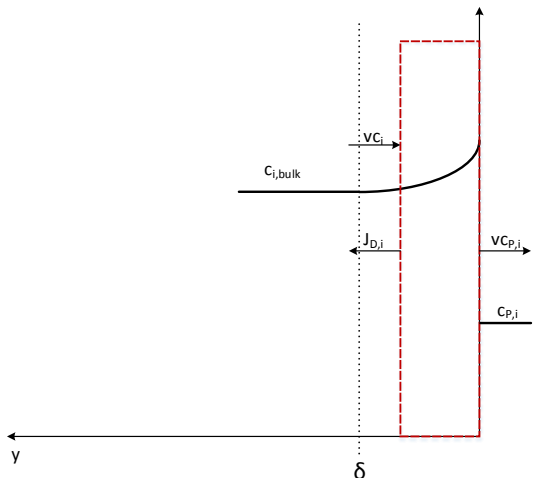

Figure 2.2: Concentration polarization: less permeable component concentration gradient adjacent to the membrane. The mass balance equation for component flux across the boundary layer is the basis of the film model description of concentration polarization.

2.1 Concentration Polarization In Liquid Separation Processes

The polarization concentration phenomenon can be by model by assuming that a thin layer of fluid (laminar regime) of thickness δ exists between the membrane surface and the well-mixed bulk solution. The concentration gradients that control concentration polarization form in this layer. This boundary layer film model oversimplifies the fluid hydrodynamics occurring in membrane modules and still contains one adjustable parameter, the boundary layer thickness. Nonetheless, this simple model can explain most of the experimental data. Based on the film model theory the mass transfer resistance is lumped in a material film of thickness δ located close to the membrane interface. In this film the mass transport mechanism is assumed to obey Fick's law while in the bulk phase the concentration in assume to be uniform. The film thickness is strongly affected by the fluid-dynamic regimes established in the system: under laminar flow it can be identified as a boundary layer while under turbulent regimes as a laminar film close to the wall.
Based on the aforementioned model the transport coefficient can be defined as:

$$k = \frac{D}{\delta} \tag{2.1}$$

where,

- D represents the diffusion coefficient of the component in the mixture;
- δ represents the mass transfer film thickness.

By performing a mass balance over the control volume shown in fig. 2.2 one has:

$$\bar{J}_{\text{Diff}} + \bar{J}_{\text{Conv}} = \bar{J}_{\text{P}} \tag{2.2}$$

which implies that the mixture is moving with a velocity v toward the membrane surface. In a scalar form equation the mass flux vc_i of each components dictates:

$$-D_i \frac{dc_i}{dy} = v(c_{p,i} - c_i) \tag{2.3}$$

By integration of eq. 2.3 over the film of thickness δ and recalling eq. 2.1 a relation between c_i, c_i^I and $c_{i,p}$ is obtained:

$$\ln\left[\frac{c_i^I - c_{p,i}}{c_i - c_{p,i}}\right] = \frac{v}{k} \tag{2.4}$$

In this case the diffusion coefficient D_i has been assumed constant over the film thickness which is not always a good approximation of the real system (see ultrafiltration). Several correlation for the estimation of the transport coefficient are available in literature regarding different membrane module geometries and fluid-dynamic conditions. These correlations, which are the analogous of the the heat transfer coefficient correlations, do not take into account the velocity profile distortion due to later flux nor the variation of physical properties within the film thickness. Even though these approximations are acceptable for reverse osmosis, it must be noticed that for ultrafiltration viscosity and diffusion coefficients can reach membrane interface values very different compared to those ones in the bulk phase. In this case eq. 2.4 must be revised using a relation useful to interpret experimental results.

2.1.1 Osmotic Effect

Due to concentration polarization effects the flux over a membrane does not vary linearly with the applied pressure. In the case of the osmotic pressure:

$$J_s = \phi(\Delta p - \Delta\pi) = \phi[\Delta p - (\pi^I - \pi_p)] \tag{2.5}$$

The osmotic pressure of the retentate side is a function of the operative pressure of the retentate side. If an increased Δp is applied a consequent increment in flux will occur. At the same time an increase in c_i^I will be notice due to the membrane rejection: the value of π^I at the membrane interface will raise consequently.
The overall effect of the operation is represented by an increased flux which is lower than in the ideal condition of absence of concentration polarization.

In the process of ultrafiltration the polarization effect is much more enhanced: increasing the retentate pressure value enhance the flux that rapidly reaches an asymptotic value which is a function of concentration and fluid-dynamics only. This be-

haviour cannot be just be explained by just making use of the osmotic effect: the most popular model is the *gel model*[1].

2.2 Concentration Polarization In Gas Separation Processes

Concentration polarization in gas separation processes has not been widely studied, but usually the effect can be assumed to be small because of the high diffusion coefficients of gases. In calculating the expression for the concentration polarization of gases, the simplifying assumption that the volume fluxes on each side of the membrane are equal cannot be made. The starting point for the calculation is the mass balance equation (eq. 2.3), which for gas permeation is written

$$J_r c_{r,i} - D_i \frac{dc_i}{dx} = J_p c_{p,i} \tag{2.6}$$

where J_r is the volume flux of gas on the feed side of the membrane and J_p is the volume flux on the permeate side. These volume fluxes (cm^3/cm^2s) can be linked by correcting for the pressure on each side of the membrane using the expression

$$J_r c_{r,i} p_r = J_p c_{p,i} p_p \tag{2.7}$$

where p_r and p_p are the gas pressures on the retentate and permate sides of the membrane.
Hence,

$$J_r \frac{p_r}{p_p} = J_r \phi = J_p \tag{2.8}$$

where ϕ is the pressure ratio $\frac{p_r}{p_p}$ across the membrane. Substituting eq. 2.8 into eq. 2.6 and rearranging gives

$$D_i \frac{c_{r,i}}{dx} = J_r(\phi c_{p,i} - c_{r,i}) \tag{2.9}$$

Integrating across the boundary layer thickness, as before, gives

$$\ln \left[\frac{\frac{c_i^I}{\phi} - c_{p,i}}{\frac{c_i}{\phi} - c_{p,i}} \right] = \frac{J_r \delta}{D_i} \tag{2.10}$$

REFERENCES

1. Baker, R.W., *Membrane Technology and Applications*, John Wiley & Sons Ltd: United Kingdom, **2012**.

[1]G. A. Denisov, Theory of concentration polarization in cross-flow ultrafiltration: gel-layer model and osmotic-pressure model, Journal of Membrane Science 91 (1994) 173-187.

CHAPTER 3

DESIGN OF GAS SEPARATION MODULES

3.1 Introduction

The separation and economic performance of a membrane-based gas separation process depend on several parameters. A correlation between input conditions, operating variables and output conditions must be clarified for the analysis to be carried out. Generally, the input conditions are given by the feed stream, while the outcome has to be intended in terms of separation and economic indicators. In the framework of gas separation, the main performance indicators are recovery (*R*), purity (*P*), and separation factor (α^*) of a given component i, given by

$$R = \frac{\dot{n}_{i,p}(L)\ y_{i,p}(L)}{\dot{n}_{i,F}\ y_{i,F}} \tag{3.1}$$

$$P = y_{i,p}(L) \tag{3.2}$$

$$\alpha^* = \frac{y_{i,p}(L)\ [1 - y_{i,r}(L)]}{y_{i,r}(L)\ [1 - y_{i,p}(L)]} \tag{3.3}$$

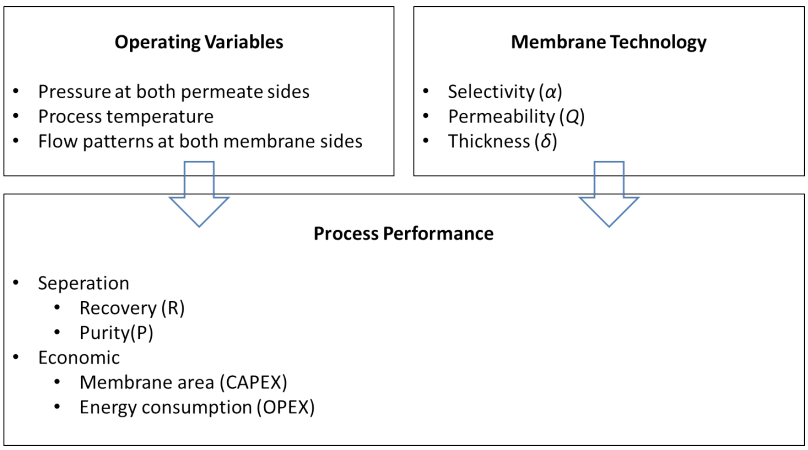

Figure 3.1: Schematic of membrane gas separation process design and evaluation.

Where $\dot{n}$ indicates the molar flow rate, y the molar fraction and L is the length of the module. The subscripts r and p refers to the component i in the retentate side or permeate side respectively. The subscript f indicates the feed stream.
On the other side the cost of a membrane process relates to the compression energy and to the membrane area. The former translates in operating cost (OPEX), while the latter in investment cost (CAPEX). Figure 3.1 displays a schematic of a membrane-based gas separation process design and evaluation. In a first place, a gas separation membrane module can be thought as a black box with 1 inlet stream: the feed, and 2 outlet streams: the retentate and the permeate.

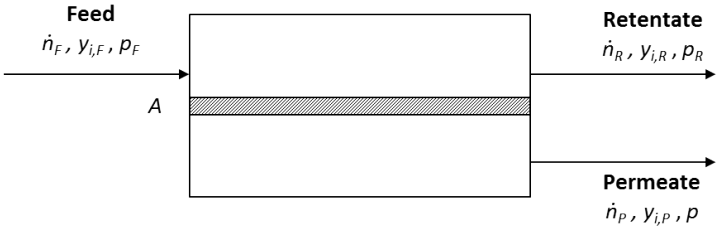

Figure 3.2: Schematic of membrane gas separation process design and evaluation.

Therefore, a general membrane-based gas separation can be described by the following equations:

- *Overall material balance equations*.

$$\dot{n}_p + \dot{n}_r = \dot{n}_f \tag{3.4}$$

- *Species i balance equations*.

$$\dot{n}_p\, y_{i,p} + \dot{n}_r\, y_{i,r} = \dot{n}_f\, y_{i,f} \qquad i = 1, ..., N_c - 1 \tag{3.5}$$

Where N_c represents the number of components of the gas mixture entering the membrane module. The material balances can be also expressed in terms of flux across the membrane. In particular,

$$\dot{n}_p = \sum_i^{N_c} \int_0^A J_i ds \tag{3.6}$$

Where J_i indicates the flux of the component i and can be expressed through the solution-diffusion model, below. The membrane area A can be expressed according to the module geometry, i.e. as a cylinder in the case of a hollow-fiber module, or a plate in the case for a spiral-wound module.

- *Flux equations*. The solution-diffusion model states,

$$J_i = \frac{Q_i}{\delta} \left(p_f\, y_{i,r} - p\, y_{i,p}\right) \tag{3.7}$$

- *Composition equations*. It should be recalled that the sum of the molar fractions must always equal the unity.

$$\sum_i^{N_c} y_{i,f} = 1 \tag{3.8}$$

$$\sum_i^{N_c} y_{i,r} = 1 \tag{3.9}$$

$$\sum_i^{N_c} y_{i,p} = 1 \tag{3.10}$$

In their pioneering work, Weller and Steiner [1] proposed two models for modeling the separation of gas binary mixture through membranes: perfect mixing on both sides, and no mixing on both sides. Afterward, Hwang and Kammermeyer [2] investigated the separation behavior of a single-stage membrane module. After them, this general design problem has been widely extended by other authors with more complex models accounting for multi-component mixtures as well as different hydrodynamic conditions and module geometries. In the following, a generic binary mixture α + β, where α is the most permeable component through the membrane, is considered. Three basic design approaches are outlined: perfect mixing, cross-plug flow and counter-current flow.

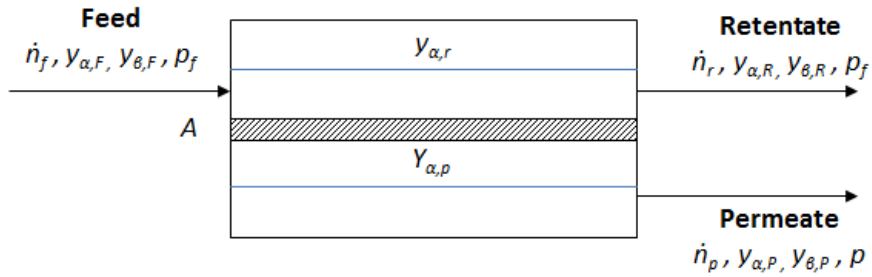

Figure 3.3: Schematic of a membrane gas separation module characterized by perfect mixing at both retentate and permeate side.

3.2 Gas Separation Module with Perfect Mixing

Figure 3.3 displays the schematic of a membrane gas separation module characterized by perfect mixing at both retentate and permeate side. p indicates the fluid pressure. The main assumption of this model is that the rate of mixing on both sides is much than the flow rate. This translates in constant composition at either sides of the membrane. The following assumption are made:

1. Mixing rate (MR) much higher than fluid velocity (u), at both sides of the membrane. This translate in constant composition profiles (blue lines in figure 3.3) equal to $y_{\alpha,r}$ and $y_{\alpha,p}$ at retentate and permeate side, respectively.
2. Isothermal process
3. Constant pressure at both sides of the membrane
4. Constant membrane properties, i.e. selectivity and permeability independent from temperature, pressure and gas composition.
5. Negligible non-idealities, such as fiber deformation, membrane swelling, membrane plasticization.

Assumption 1 can be interpreted as non-moving fluid inside the membrane. The equations below can be written when dealing with a membrane gas separation module. The permeate and retentate quantities refer to the section L. For sake of simplicity this is implied in the section.

- *Material balance equations*.

$$\dot{n}_p \, y_{\alpha,p} + \dot{n}_r \, y_{\alpha,r} = \dot{n}_f \, y_{\alpha,f} \tag{3.11}$$

$$\dot{n}_p \, y_{\beta,p} + \dot{n}_r \, y_{\beta,r} = \dot{n}_f \, y_{\beta,f} \tag{3.12}$$

The material balances can be also expressed in terms of flux across the membrane.

$$J_\alpha \, A = \dot{n}_p \, y_{\alpha,p} \tag{3.13}$$

$$J_\beta \, A = \dot{n}_p \, y_{\beta,p} \tag{3.14}$$

It must be noted that the material balances can be expressed either for the two components or for one component and the overall mixture.

- *Flux equations*. The flux across the membrane, J, is expressed by mean of the solution-diffusion model. The driving force across the membrane, provided by the partial pressure gradient at the sides of the membrane, is constant due to the flat composition profiles.

$$J_\alpha = \frac{Q_\alpha}{\delta} \left(p_f \, y_{\alpha,r} - p \, y_{\alpha,p} \right) \tag{3.15}$$

$$J_\beta = \frac{Q_\beta}{\delta} \left(p_f \, y_{\beta,r} - p \, y_{\beta,p} \right) = \frac{Q_\beta}{\delta} \left[p_f \, (1 - y_{\alpha,r}) - p \, (1 - y_{\alpha,p}) \right] \tag{3.16}$$

Where Q indicates the permeability of a given component and δ the thickness of the membrane. The membrane area A can be expressed according to the module geometry, i.e. as a cylinder in the case of a hollow-fiber module, or a plate in the case for a spiral-wound module.

- *Composition equations*. The sum of the molar fractions must equal the unity.

$$y_{\alpha,r} + y_{\beta,r} = 1 \tag{3.17}$$

$$y_{\alpha,p} + y_{\beta,p} = 1 \tag{3.18}$$

The aforementioned equations systems is solved to determine the performance of the membrane module. The system includes 8 linearly independent equations: 3.11 - 3.18, and 10 unknowns: $\dot{n}_r$, $\dot{n}_p$, $y_{\alpha,r}$, $y_{\alpha,p}$, $y_{\beta,r}$, $y_{\beta,p}$, J_α, J_β, p, A. The feed conditions, $\dot{n}_f$, $y_{\alpha,f}$, p_f, are assumed to be known. Therefore, the system still presents two degrees of freedom. This implies that two variables must be fixed to complete the module design.
In common practice, some dimensionless parameter are introduced in the analysis. In particular, the stage cut, θ, defines the ratio of permeate to feed flow rate; the pressure ratio, β, indicates the ratio of permeate to feed pressure; the membrane selectivity, α, is the ratio of most permeant to least permeant component permeabilities, i.e. $\alpha > 1$.

$$\alpha = \frac{Q_\alpha}{Q_\beta} \tag{3.19}$$

$$\beta = \frac{p}{p_f} \tag{3.20}$$

$$\theta = \frac{\dot{n}_p}{\dot{n}_f} \tag{3.21}$$

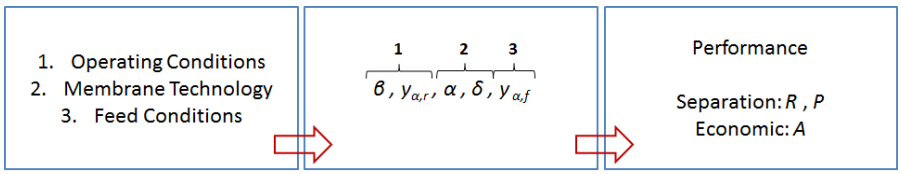

Figure 3.4: Simplified schematic of membrane performance evaluation for the design of a perfect mixing module.

By re-arranging equations 3.13 - 3.16, the membrane area can be expressed as a function of stage cut, molar fractions, membrane technology and operating variables.

$$A = \frac{y_{\alpha,p}\,\dot{n}_p}{J_\alpha} = \frac{y_{\alpha,p}\,\theta\,\dot{n}_f}{\frac{Q_\alpha}{\delta}\,(p_f\,y_{\alpha,r} - p\,y_{\alpha,p})} \tag{3.22}$$

By expressing the recovery as a function of the stage cut

$$R = \frac{\dot{n}_{\alpha,p}\,y_{\alpha,p}}{\dot{n}_{\alpha,f}\,y_{\alpha,f}} = \theta\,\frac{y_{\alpha,p}}{y_{\alpha,f}} \tag{3.23}$$

equation 3.22 can be written as

$$A = \frac{y_{\alpha,p}\,\dot{n}_p}{J_\alpha} = \frac{R\,\dot{n}_f\,y_{\alpha,f}}{\frac{Q_\alpha}{\delta}\,(p_f\,y_{\alpha,r} - p\,y_{\alpha,p})} \tag{3.24}$$

The objective of the membrane design is to define a procedure so that given the operating conditions, the membrane technology, and the feed conditions, the membrane performance is determined. In this simple case:

$$(P, R, A) = f\,(\beta, y_{\alpha,r}, \alpha, \delta, y_{\alpha,f}) \tag{3.25}$$

Figure 3.4 illustrates a schematic of such a procedure. As mentioned above, two variables must be fixed in this context. In fact, these change with the investigated application. For instance, in the context of CO_2 / N_2 separation, the permeate requirements are usually specified; on the other hand, when dealing with biogas upgrading, CO_2 / CH_4 separation, the retentate side is provided as a process specification. In both cases the economic performance can be calculated.

By dividing equation 3.15 by 3.16, and using equations 3.15 - 3.16, 3.17 - 3.18 it is possible to write

$$\frac{J_\alpha}{J_\beta} = \frac{Q_\alpha\,(p_f\,y_{\alpha,r} - p\,y_{\alpha,p})}{Q_\beta\,[p_f\,(1 - y_{\alpha,r}) - p\,(1 - y_{\alpha,p})]} = \frac{\dot{n}_p\,y_{\alpha,p}}{\dot{n}_p\,y_{B,p}} = \frac{y_{\alpha,p}}{1 - y_{\alpha,p}} \tag{3.26}$$

Introducing α and β,

$$\frac{y_{\alpha,p}}{1 - y_{\alpha,p}} = \alpha\frac{y_{\alpha,r} - \beta\,y_{\alpha,p}}{(1 - y_{\alpha,r}) - \beta\,(1 - y_{\alpha,p})} \tag{3.27}$$

Equation 3.27 can be re-arranged as a quadratic expression of $y_{\alpha,p}$, which corresponds to the purity of the product.

$$\beta\,(\alpha-1)\,y_{\alpha,p}^2-[1+(\alpha-1)\,(\beta+y_{\alpha,r})]\,y_{\alpha,p}-\alpha\,y_{\alpha,r}=0 \tag{3.28}$$

The physical solution of the second-degree equation can be expressed in the general form

$$y_{\alpha,p}=\frac{-b-\sqrt{b^2-4\,a\,c}}{2\,a} \tag{3.29}$$

Where,

$$a=\beta\,(\alpha-1) \tag{3.30}$$
$$b=-\,[1+(\alpha-1)\,(\beta+y_{\alpha,r})] \tag{3.31}$$
$$c=\alpha\,y_{\alpha,r} \tag{3.32}$$

$y_{\alpha,p}$ can be calculated by assigning the pressure ratio, β, the retentate molar fraction, $y_{\alpha,r}$ and the membrane technology, α. Once the molar fractions are known, the molar flow rates, and thus the recovery, can be determined through the material balance equations, i.e. equations 3.11 - 3.12. Finally, the membrane area is determined through the flux equation. It must be noted that, similarly, the membrane area could be fixed and the recovery / purity calculated. This implies a choice between economic and separation performance.
As mentioned above, in different situations the retentate conditions represent the calculation outcome, with fixed permeate conditions. In this case, the equations above can be re-arranged to obtain a first-order expression of $y_{\alpha,r}$.

$$y_{\alpha,r}=\frac{y_{\alpha,p}\;[\alpha\,(y_{\alpha,p}-1)-\beta+1-y_{\alpha,p}]}{y_{\alpha,p}\,\beta(\alpha-1)-\alpha\,\beta} \tag{3.33}$$

Finally, it must be stressed that the same procedure could be followed for a multicomponent separation system. In this case, the system would be composed by 3 N_{comp} + 3 equations, and by a corresponding number of unknowns, being N_{comp} the number of components.
In fact, more realistic flow patterns are used to investigate the performance of a membrane-based separation process. Depending on the complexity, they may require a numerical solution. In the following, two examples of more realistic module configurations are given.

3.3 Gas Separation Module with Cross-plug flow

Membrane separation models have been developed for a wide range of hydrodynamic conditions. The previous section depicted an ideal case, where perfect mixing occurs at both side of the membrane, i.e. the simplest case that can be considered. The present section deals with the cross-plug flow model. A one-dimensional

concentration profile is considered at the retentate side; contemporary, the fluid is assumed to be collected immediately from the permeate side. As a consequence, although the permeate molar fraction depends on the flow at the retentate side, it is independent of the the flow at the permeate side. The symbol $y'_{\alpha,p}$ is used to indicate the value of the permeate molar fraction along the membrane module, depending on the retentate conditions. On the other hand, $y_{\alpha,p}$ indicates the value at the membrane output, calculated from a global material balance on the membrane module. The cross-plug flow model remains a cornerstone in the membrane field, mainly because it realistically predicts the separation performance of a hollow-fiber module under a significant pressure ratio [3]. Figure 3.5 illustrates a schematic of a membrane gas separation module characterized by a cross-plug flow. Assumptions 2 to 5 are maintained and a binary mixture $\alpha + \beta$ is taken into account. In this framework, the proposed methodology holds for any type of flow pattern. Referring to figures 3.6 - 3.5 the following equations can be written.

- *Material balance equations*. First, the overall material balance on the membrane module is written. These equations define the conditions at the end of the membrane module ($z = L$).

$$\dot{n}_p + \dot{n}_r(L) = \dot{n}_f \tag{3.34}$$

$$\dot{n}_p \, y_{\alpha,p} + \dot{n}_r(L) \, y_{\alpha,r}(L) = \dot{n}_f \, y_{\alpha,f} \tag{3.35}$$

  The material balances can be written for the differential element dz (at retentate side) indicated by the red dashed line in the figure.

$$d\dot{n}_r = -J \, ds \tag{3.36}$$

$$d(\dot{n}_r \, y'_{\alpha,r}) = -J \, y'_{\alpha,p} \, ds \tag{3.37}$$

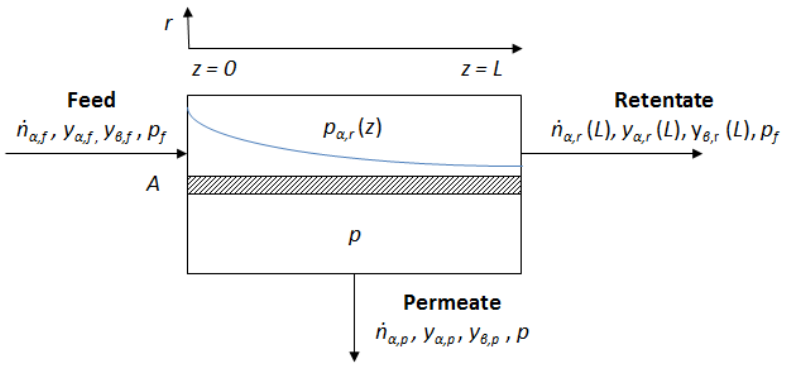

Figure 3.5: Schematic of membrane gas separation module characterized by a cross-plug flow.

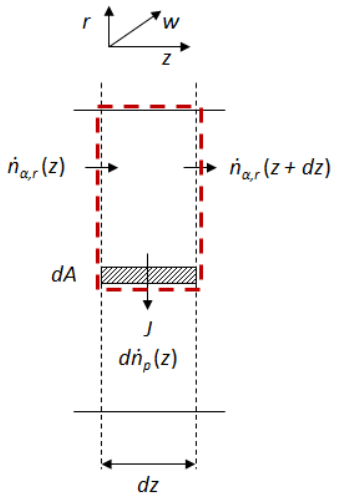

Figure 3.6: Differential element dz within the cross-plug membrane module.

Where the minus sign indicates that a positive flux corresponds to a reduction in the retentate flow rate, due to the material permeation across the membrane. The membrane area coordinate s is proportional to z with a relationship that depends on the membrane geometry. In particular, for a cylindrical or plane geometry, the membrane area can be expressed as follows,

- *Plate geometry*: $ds = W\ dz$
- *Cylinder geometry*: $ds = \pi\ D_o\ dz$

Where W indicates the width of the membrane plate and D_o the outer radius of the cylinder membrane.

- *Flux equations*. The flux is expressed through the solution-diffusion model.

$$J\ y'_{\alpha,p}(z) = \frac{Q_\alpha}{\delta}\ \left[p_f\ y_{\alpha,r}(z) - p\ y'_{\alpha,p}(z)\right] \tag{3.38}$$

$$J\ \left[1 - y'_{\alpha,p}(z)\right] = \frac{Q_\beta}{\delta}\ \left[p_f\ \left[1 - y_{\alpha,r}(z)\right] - p\ \left[1 - y'_{\alpha,p}(z)\right]\right] \tag{3.39}$$

Where the composition equations 3.17 - 3.18 are included. Here, the stoichiometric equations $y_{\alpha,r} + y_{\beta,r} = y_{\alpha,p} + y_{\beta,p} = y'_{\alpha,p} + y'_{\beta,p} = 1$ are implied for any z along the membrane.

The aforementioned equation system is solved to determine the performance of the membrane module. The system includes six equations: 3.34 - 3.39, and eight variables: $\dot{n}_r$, $\dot{n}_p$, $y_{\alpha,r}$, $y_{\alpha,p}$, $y'_{\alpha,p}$, J, p, A. The feed conditions are assumed to be given: $\dot{n}_f$, $y_{\alpha,f}$, p_f, also providing for the boundary conditions for the differential

equations. It is worth noting, one more time, that the system presents two degrees of freedom.

Although correctly formulated, the set of equations 3.34-3.39 can be manipulated in order to obtain a dimensionless and more responsive system of equations. One of the possible manipulations is described by the procedure in the following.
By dividing equation 3.38 by equation 3.39, the algebraic expression stated by 3.27 can be obtained. However, it now has to be intended as a local expression, holding for any generic section z. Hereafter, the local nature of the molar fractions and mole flow rates will be implied for notation simplicity. Re-arranging,

$$y'_{\alpha,p} = \frac{1+(\alpha-1)\ (\beta+y_{\alpha,r})-\sqrt{[1+(\alpha-1)\ (\beta+y_{\alpha,r})]^2-4\ \alpha\ \beta\ (\alpha-1)\ y_{\alpha,r}}}{2\ \beta\ (\alpha-1)} \tag{3.40}$$

It is worth noticing that $y'_{\alpha,p}$ can be expressed uniquely as a function of α, β, $y_{\alpha,r}$.
Moreover, by combining equations 3.36 and 3.38, it is possible to write:

$$d(\dot{n}_r) = -Jds = -\frac{y_{\alpha,r} - \beta\ y'_{\alpha,p}}{y'_{\alpha,p}}\ \left(\frac{Q_\alpha\ p_f\ ds}{\delta}\right) \tag{3.41}$$

Next, the following dimensionless quantities are introduced:

$$\sigma = \frac{Q_\alpha\ p_f\ s}{\delta\ \dot{n}_f} \tag{3.42}$$

$$\psi = \frac{\dot{n}_r}{\dot{n}_f} \tag{3.43}$$

$$\theta = \frac{\dot{n}_p}{\dot{n}_f} \tag{3.44}$$

$$\Phi = J\ \frac{s}{\dot{n}_f} \tag{3.45}$$

Defining the dimensionless membrane area coordinate (σ), the dimensionless retentate mole flow rate (ψ), the dimensionless permeate flow rate (θ), and the dimensionless flux (Φ), respectively.
Equation 3.41 can be written in dimensionless form:

$$d\psi = -\frac{y_{\alpha,r} - \beta\ y'_{\alpha,p}}{y'_{\alpha,p}}\ d\sigma \tag{3.46}$$

Depicting an ordinary differential equation relating the dimensionless mole flow rate with the dimensionless area.
Equation 3.36 can be used in equation 3.37 to derive the following expression,

$$d(\dot{n}_r\ y_{\alpha,r}) = y'_{\alpha,p}\ d\dot{n}_r \tag{3.47}$$

The definition of product differentiation can be applied to determine a correlation between the retentate molar fraction ($y_{\alpha,r}$) and the retentate mole flow rate ($\dot{n}_r$). In specific,

$$d(\dot{n}_r\ y_{\alpha,r}) = \dot{n}_r\ dy_{\alpha,r} + y_{\alpha,r}\ d\dot{n}_r = y'_{\alpha,p}\ d\dot{n}_r$$
$$dy_{\alpha,r} = -\left(y_{\alpha,r} - y'_{\alpha,p}\right)\ \frac{d\dot{n}_r}{\dot{n}_r}$$
$$\frac{dy_{\alpha,r}}{d\dot{n}_r} = -\frac{y_{\alpha,r} - y'_{\alpha,p}}{\dot{n}_r} \tag{3.48}$$

Although not of primary relevance for the purposes of the class, it is worth noticing that equation 3.48 can be integrated by parts. Indeed,

$$\frac{dy_{\alpha,r}}{y_{\alpha,r} - y'_{\alpha,p}} = -dln\ \dot{n}_r$$
$$\int_{y_{\alpha,f}}^{y_{\alpha,r}} \frac{dy_{\alpha,r}}{y_{\alpha,r} - y'_{\alpha,p}} = ln\left(\frac{\dot{n}_f}{\dot{n}_r}\right) \tag{3.49}$$

By using the definition of ψ in equation 3.48,

$$dy_{\alpha,r} = -\left(y_{\alpha,r} - y'_{\alpha,p}\right)\ \frac{d\psi}{\psi} \tag{3.50}$$

Eventually, by combining equations 3.46-3.50 an ordinary differential equation relating $y_{\alpha,r}$ with σ can be derived,

$$\frac{dy_{\alpha,r}}{d\sigma} = \frac{\left(y_{\alpha,r} - y'_{\alpha,p}\right)\ \left(y_{\alpha,r} - \beta\ y'_{\alpha,p}\right)}{y'_{\alpha,p}\ \psi} \tag{3.51}$$

As a consequence, the final set of equations can be written as follows,

$$\frac{dy_{\alpha,r}}{d\sigma} = \frac{\left(y_{\alpha,r} - y'_{\alpha,p}\right)\ \left(y_{\alpha,r} - \beta\ y'_{\alpha,p}\right)}{y'_{\alpha,p}\ \psi} \tag{3.52}$$

$$\frac{d\psi}{d\sigma} = -\frac{y_{\alpha,r} - \beta\ y'_{\alpha,p}}{y'_{\alpha,p}} \tag{3.53}$$

$$y'_{\alpha,p} = \frac{1+(\alpha-1)\ (\beta+y_{\alpha,r})-\sqrt{[1+(\alpha-1)\ (\beta+y_{\alpha,r})]^2-4\ \alpha\ \beta\ (\alpha-1)\ y_{\alpha,r}}}{2\ \beta\ (\alpha-1)} \tag{3.54}$$

$$\theta = 1 - \psi(L) \tag{3.55}$$

$$y_{\alpha,p} = \frac{y_{\alpha,f} - \psi(L)\ y_{\alpha,r}(L)}{1 - \psi(L)} \tag{3.56}$$

$$\Phi = -\frac{y_{\alpha,r} - \beta\ y'_{\alpha,p}}{y'_{\alpha,p}}\ \left(\frac{Q_\alpha\ p_f\ s}{\delta\ U_f}\right) \tag{3.57}$$

Where equations 3.55 and 3.56 are obtained from 3.34 and 3.35. The boundary conditions, in $\sigma = 0$, for the two differential equations 3.52-3.53 are the following:

$$y_{\alpha,r}(\sigma = 0) = y_{\alpha,f} \tag{3.58}$$

$$\psi(\sigma = 0) = 1 \tag{3.59}$$

For given membrane technology (α, Q, δ) and feed conditions ($\dot{n}_f$, $y_{\alpha,f}$, p_f), there are eight variables ($y_{\alpha,r}$, $y_{\alpha,p}$, $y'_{\alpha,r}$, β, σ, Φ, ψ, θ) to satisfy six equations. This implies the any of these two variables may be specified.

3.4 Gas Separation Module with Counter-current Flow

A counter-current membrane module, displayed in figure 3.7 is investigated. The figure highlights the qualitative composition profile along the module (blue lines). Hence, it illustrates how the counter-current configuration is beneficial in terms of maximization of the driving force for any section z. At this point, it is clear that the material flux across the membrane is proportional to the partial pressure difference at the membrane sides:

$$J_i \propto p_{i,f} - p_i \tag{3.60}$$

Therefore, the partial pressure gradient is maximized in every section:

$$@ \ z = 0, \ p_{i,r} = p_{i,f}, \ p_i = p_{i,max}$$
$$@ \ z = L, \ p_{i,r} = p_{i,r,min}, \ p_i = 0$$

Assumptions 2 - 5 stated in section 3.2 holds true and a binary mixture A + B is considered. However, differently from the previous cases, the flux depends on both retentate and permeate conditions. A one-dimensional concentration profile is presumed at both side of the membrane. Therefore, constant composition is considered in the radial direction. Referring to figure 3.8 the following equations can be written.

- *Overall material balance equations*. First, the overall material balances on the membrane module is written.

$$\dot{n}_p \ y_{\alpha,p} + \dot{n}_r(L) \ y_{\alpha,r}(L) = \dot{n}_f \ y_{\alpha,f} \tag{3.61}$$

$$\dot{n}_p(L) \ [1 - y_{\alpha,p}(L)] + \dot{n}_r(L) \ [y_{\alpha,r}(L)] = \dot{n}_f \ (1 - y_{\alpha,f}) \tag{3.62}$$

  Where the composition equations are again implied, being the two molar fractions complementary: $y_{\alpha,r} + y_{B,r} = y_{\alpha,p} + y_{B,p} = y_{\alpha,f} + y_{B,f} = 1$.

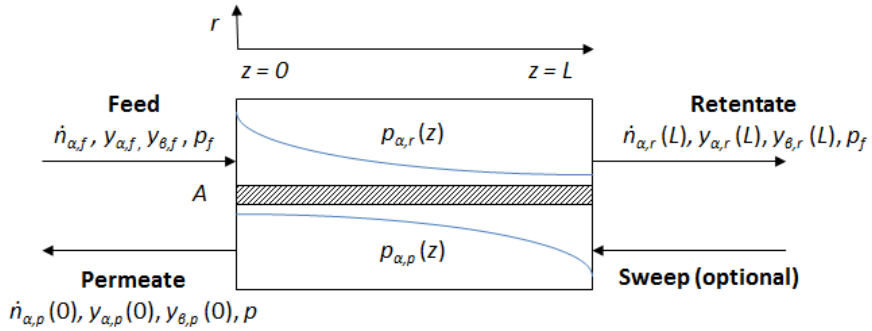

Figure 3.7: Schematic of membrane gas separation module characterized by counter-current flow.

- *Differential material balance equations*. The material balances can be referred to the differential element indicated by the dashed red line in figure 3.8. Note that in this case the differential element includes both the retentate and the permeate side.

$$\dot{n}_r(z)\, y_{\alpha,r}(z) + \dot{n}_p(z+dz)\, y_{\alpha,p}(z+dz) = \dot{n}_r(z+dz)\, y_{\alpha,r}(z+dz) + \dot{n}_p(z)\, y_{\alpha,p}(z) \tag{3.63}$$

$$\dot{n}_r(z)\ [1 - y_{\alpha,r}(z)] + \dot{n}_p(z+dz)\ [1 - y_{\alpha,p}(z+dz)] = \dot{n}_r(z+dz)\ [1 - y_{\alpha,r}(z+dz)] + \dot{n}_p(z)\ [1 - y_{\alpha,p}(z)] \tag{3.64}$$

Equations 3.63 and 3.64 can written in differential form as

$$d(\dot{n}_r\, y_{\alpha,r}) = d(\dot{n}_p\, y_{\alpha,p}) \tag{3.65}$$

$$d\left[\dot{n}_r\ (1 - y_{\alpha,r})\right] = d\left[\dot{n}_p\ (1 - y_{\alpha,p})\right] \tag{3.66}$$

- *Flux equations*. The flux is expressed by mean of the solution-diffusion model. Both retentate and permeate flow rates could equally be computed in the definition of the membrane flux. In the following, the retentate flow rate is considered.

$$\frac{d(\dot{n}_r\, y_{\alpha,r})}{ds} = \frac{d(\dot{n}_p\, y_{\alpha,p})}{ds} = -\frac{Q_\alpha}{\delta}\ [p_f\, y_{\alpha,r}(z) - p\, y_{\alpha,p}(z)] \tag{3.67}$$

$$\frac{d\left[\dot{n}_r\ (1 - y_{\alpha,r})\right]}{ds} = \frac{d\left[\dot{n}_p\ (1 - y_{\alpha,p})\right]}{ds} = -\frac{Q_\beta}{\delta}\ [p_f\ [1 - y_{\alpha,r}(z)] - p\ [1 - y_{\alpha,p}(z)]] \tag{3.68}$$

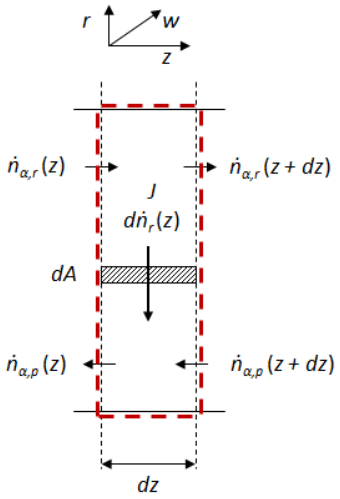

Figure 3.8: Differential element dz within the counter-current membrane module.

The feed conditions, $\dot{n}_f$, $y_{\alpha,f}$, p_f, which also provides the boundary conditions for the differential equations, are assigned. The equations system presented above can be re-arranged in a set of 4 linearly independent equations with 6 unknowns. As a consequence, two degrees of freedom can be specified for the design problem. One possibility for re-organizing the aforementioned equations leads to a system composed by equations 3.62 - 3.61 and completed by,

$$\dot{n}_r \frac{dy_{\alpha,r}}{ds} = \\ = \frac{y_{\alpha,r} - y_{\alpha,p}}{y_{\alpha,p} - y_{\alpha,f}} \left[(1 - y_{\alpha,r}) \, Q' \alpha \, (p_f \, y_{\alpha,r} - p \, y_{\alpha,p}) - \right. \\ \left. y_{\alpha,r} \, Q' \beta \, [p_f \, (1 - y_{\alpha,r}) - p \, (1 - y_{\alpha,p})] \right] \tag{3.69}$$

$$\dot{n}_r \frac{dy_{\alpha,p}}{ds} = \\ \frac{y_{\alpha,r} - y_{\alpha,p}}{y_{\alpha,r} - y_{\alpha,f}} \left[(1 - y_{\alpha,p}) \, Q' \alpha \, (p_f \, y_{\alpha,r} - p \, y_{\alpha,p}) - \right. \\ \left. y_{\alpha,p} \, Q' \beta \, [p_f \, (1 - y_{\alpha,r}) - p \, (1 - y_{\alpha,p})] \right] \tag{3.70}$$

Where both retentate and permeate properties must be intended as local quantities, function of the independent coordinate z. The presented equations differ from those solving the co-current flow case only in the fact that $y_{\alpha,r}$ and $\dot{n}_r$ are replaced by $y_{\alpha,f}$ and $\dot{n}_f$, respectively. The system can be solved by providing two specifications, concerning either separation performance or energy consumption and membrane area. A solving approach for a membrane module characterized by co-current flow is presented in appendix A.

3.5 Design Considerations

3.5.1 Membrane Technology

As previously mentioned, operating variables and membrane technology are the two principal components in the design of a membrane-based gas separation process. Concerning the technology, two main properties are involved in the analysis: membrane permeability, Q_i, and membrane selectivity, $\alpha_{i,j}$. The former indicates the ability of the membrane to permeate a gas, and refers to a given component i. The latter indicates the ability of the membrane in separating the species i from a mixture of two gases i + j, and thus refers to a couple of components i and j. These two properties are given, respectively, by:

$$Q_i = D_i \, K_i \tag{3.71}$$

$$\alpha_{i,j} = \frac{Q_i}{Q_j} = \left(\frac{D_i}{D_j}\right)\left(\frac{K_i}{K_j}\right) \tag{3.72}$$

D_i is the permeate diffusion coefficient (expressed in cm^2 / s), which is a measure of the mobility of individuals molecules in the membrane; K_i is the sorption coefficient (expressed in ${\mathrm{cm_i}}^3/{\mathrm{cm_{pol}}}^3$). The term D_i/D_j, the ratio of the diffusion coefficients of the two gases, represents the mobility selectivity, reflecting the different size and shape of the two molecules; K_i/K_j, the ratio of the sorption coefficients, can be viewed as the sorption selectivity, reflecting the relative solubility of the two gases in the membrane material. It should be stressed that all membrane-based gas separation commercial applications involve polymeric materials. Furthermore, despite the synthesis and evaluation of hundreds of new materials, more than 90 percent of current commercial membranes are made from less than 10 materials, most of which have been in used for decades.

- In all polymers, the *diffusion coefficient* decreases with increasing permeant molecular size. Indeed, large molecules interact with more segments of the polymer chain than do small molecules. Hence, the mobility selectivity always favors the passage of small molecules over large ones [1]. However, the magnitude of the mobility selectivity term depends significantly on whether the membrane is above or below the glass transition temperature, T_g. When a material is below such a temperature, the polymer chains are basically fixed and segmental motion is limited. The material is then called a glassy polymer, being tough and rigid. Above the glass transition temperature, the segments of the polymer chains have sufficient thermal energy to allow limited rotation around the chain backbone. This motion changes remarkably the mechanical properties of the material, which becomes a rubber. The relative mobility of gases differs significantly in rubbers and glasses, as depicted in figure 3.9, from [1]. The figure shows how the diffusion coefficient in glassy materials is small and decrease more rapidly with the permeant size than in rubber materials. This implies a smaller mobility selectivity for rubbery membranes than for glassy polymers.

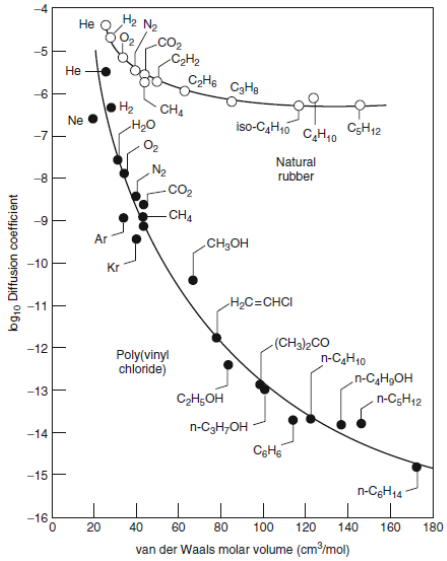

Figure 3.9: Diffusion coefficient as a function of molar volume for a variety of permeants in rubber and glassy polymers, [1].

- The *sorption coefficient* increases with increasing condensability of the permeant. This dependence on condensability turns into a dependence on molecular diameter, because larger molecules are usually more condensable than smaller ones. Figure 3.10 displays the sorption coefficient plotted against the molecular volume. The figure states that the sorption selectivity favors larger, more condensable molecules. However, contrarily to diffusion coefficient, the sorption coefficient is essentially constant in a wide range of chemically different polymers. This is because gas sorption in most polymers behaves as though the polymers were ideal liquid: It can be shown that all the ideal liquids should have the same sorption for the same gas.

As a consequence, the balance between the diffusion coefficient and the sorption coefficient, and therefore the permeability, is different for glassy and rubbery polymers. The difference is illustrated by figure 3.11, presenting the balance between sorption and diffusion in rubbery and glassy polymers. The natural rubber membranes are highly permeable; permeability increases rapidly with increasing permeant size because sorption dominates. The glass membranes are much less permeable; the permeability decreases with increasing permeant size because diffusion dominates.

Permeability and selectivity properties of polymers membranes for a number of the most important gas separation applications have been summarized by Robeson [6]. The Robeson plot, depicting membrane selectivity versus membrane permeability, represents an important tool in preliminary gas separation membrane mod-

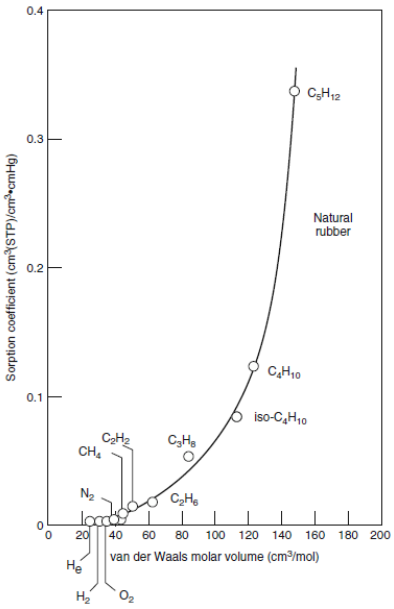

Figure 3.10: Sorption coefficient as a function of molecular volume for natural rubber membranes, [1].

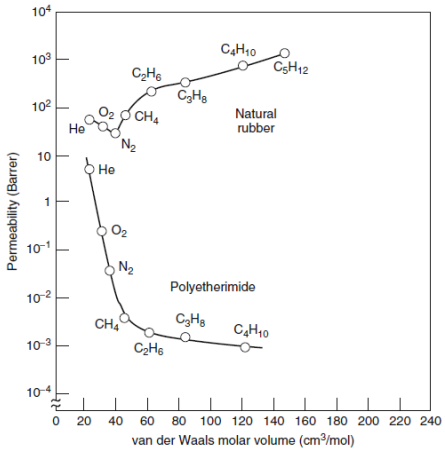

Figure 3.11: Permeability as a function of molar volume for a rubbery and a glassy polymers, [1].

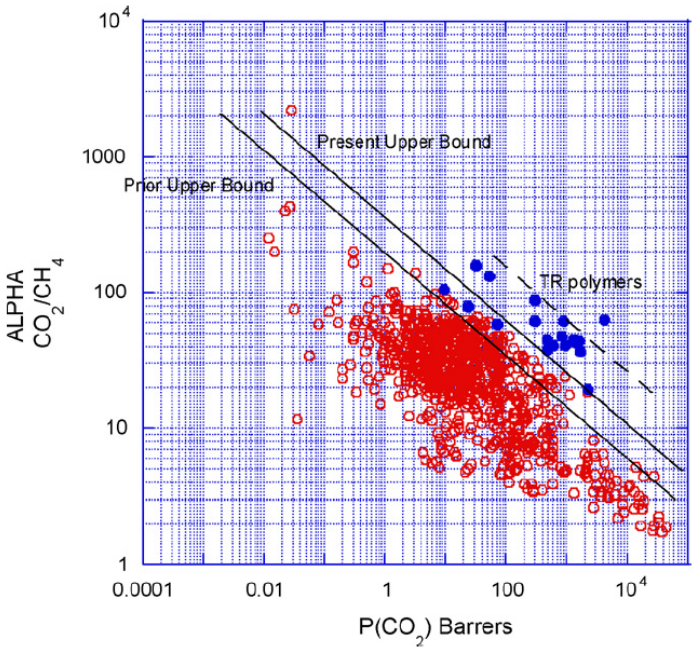

Figure 3.12: Upper bound correlation for CO_2/CH_4 separation (TR, thermally rearranged polymers), [6].

ule design. An example of the Robeson plot for the separation of carbon dioxide and methane is presented in figure 3.12. Such a separation currently finds industrial applications in the context of biogas upgrading. However, it is worth noting that the Robeson plot reports membrane properties based on pure gas measurements at ambient pressure and temperature. However, the actual value of selectivity and permeability for mixtures, at real industrial conditions, decreases significantly [7].

3.5.2 Operating Variables

Followng Baker's dissertation presented in [1], some considerations can be done concerning a membrane-based gas separation process. Recalling the definition of the flux across the membrane,

$$J_i(z) = \frac{Q_i}{\delta}\left[p_f\, y_{i,r}(z) - p\, y_{i,p}(z)\right] \tag{3.73}$$

it is possible to note that $y_{i,r}(z)\, p_f > y_{i,p}(z)\, p, \forall z$ must hold, in order to have $J_i > 0$. This translate in the condition

$$\frac{y_{i,r}(z)}{y_{i,p}(z)} \leq \frac{P}{p_f} = \beta,\ \forall z \implies \frac{y_{i,p}(z)}{y_{i,r}(z)} \leq \frac{1}{\beta} = \gamma,\ \forall z \tag{3.74}$$

This implies that the maximum achievable separation is limited by the ratio between the retentate to the permeate pressure, indicated as γ.
Assuming a well-mixed configuration, with constant concentration profiles at both sides of the membrane, equation 3.29 can be derived. Re-writing the equation in terms of γ rather than β, a new expression can be obtained:

$$y_{\alpha,p} = \frac{\gamma}{2} \left[y_{\alpha,f} + \frac{1}{\gamma} + \frac{1}{\alpha-1} - \sqrt{\left(y_{\alpha,f} + \frac{1}{\gamma} + \frac{1}{\alpha-1} \right)^2 - \frac{4\ \alpha\ y_{\alpha,f}}{(\alpha-1)\ \gamma}} \right] \tag{3.75}$$

Expression 3.75 can be seen as composed by two limiting cases depending on the relative magnitude of γ and α. First, if the membrane selectivity is much larger than the ratio of retentate to permeate pressure, $\alpha >> \gamma = 1/\beta$, then the expression can be simplified as

$$y_{\alpha,p} = y_{\alpha,r}\ \gamma \tag{3.76}$$

This is the so-called pressure ratio-limited region. In this region, the difference between retentate and permeate sides is so small compared to the membrane selectivity that the membrane performance is determined solely by the pressure ratio across the membrane, independently from the selectivity.
On the other hand, if the membrane selectivity is much smaller than the ratio of retentate to permeate pressure, $\alpha << \gamma = 1/\beta$, then expression 3.75 becomes (after some manipulation and the application of l'Hôpital's rule),

$$y_{\alpha,p} = \frac{\alpha\ y_{\alpha,r}}{y_{\alpha,r}\ (\alpha - 1) + 1} \tag{3.77}$$

This is the so-called selectivity-limited region. In this region, the membrane selectivity is so small that the separation performance is determined only by the selectivity, independently from the pressure ratio. Of course, an intermediate region between these two extreme cases is also present, where both pressure ratio and membrane selectivity have a certain influence on the performance. Figure 3.13 illustrates these three regions for a vapor/nitrogen separation, in which the calculated permeate vapor molar fraction, $y_{\alpha,p}$ is plotted versus the ratio of retentate to permeate pressure, γ, for a membrane with a vapor / nitrogen selectivity of 30 [1]. Similarly, figure 3.14 reports the same regions as a function of the membrane selectivity, for a given pressure ratio of 20. As a matter of fact, the relationship between pressure ratio and selectivity is relevant because reflecting the trade-off between compression energy and membrane area, i.e. operational and investment costs. Typical pressure ratios are in the range of 5 - 20. Figure 3.14 states that if significant improvements can be attained by increasing the selectivity from 10 to 20, negligible improvements are obtained for a selectivity larger than 100.

Finally, it is worth noticing that different correlations exist between operating variables, namely pressure ratio, membrane selectivity, membrane area, and membrane separation performance, namely recovery and purity. Figure 3.15 shows the

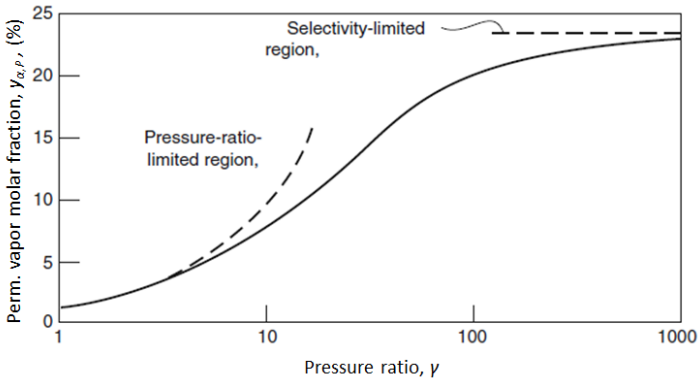

Figure 3.13: Calculated permeate vapor molar fraction for a membrane with vapor/nitrogen selectivity α = 30 and a feed molar fraction $y_{\alpha,f}$ = 0.01 as a function of the pressure ratio [1].

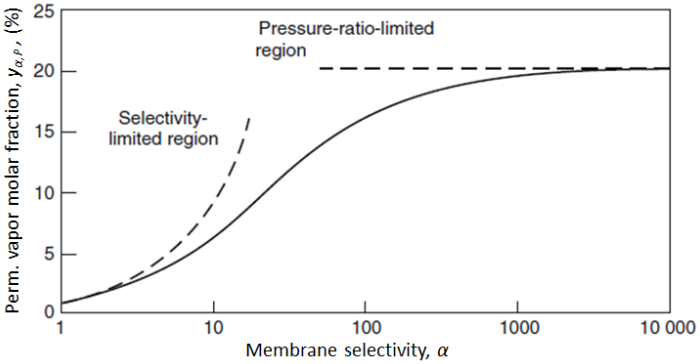

Figure 3.14: Calculated permeate vapor molar fraction for a pressure ratio β = 20 and a feed molar fraction $y_{\alpha,f}$ = 0.01 as a function of the membrane selectivity [1].

recovery and purity maps (iso-lines) on the A - β plane for two exemplary cases, with α = 30 and α = 50. Few basic conclusions can be drawn:

- Recovery and purity have opposite behaviors against the membrane area. In specific, recovery increases while purity decreases by increasing the area. This is due to the permeation of the least permeant component along the module, responsible for a degradation of the permeate purity.
- An increase (decrease) in selectivity (permeability) leads to an increase (decrease) in purity (recovery) (negative slope of the Robeson's upper bound).
- For high selectivity and high pressure ratio the permeate purity is almost independent from the membrane area. On the contrary, for low selectivity and pressure ratio the purity is almost independent from the pressure ratio.

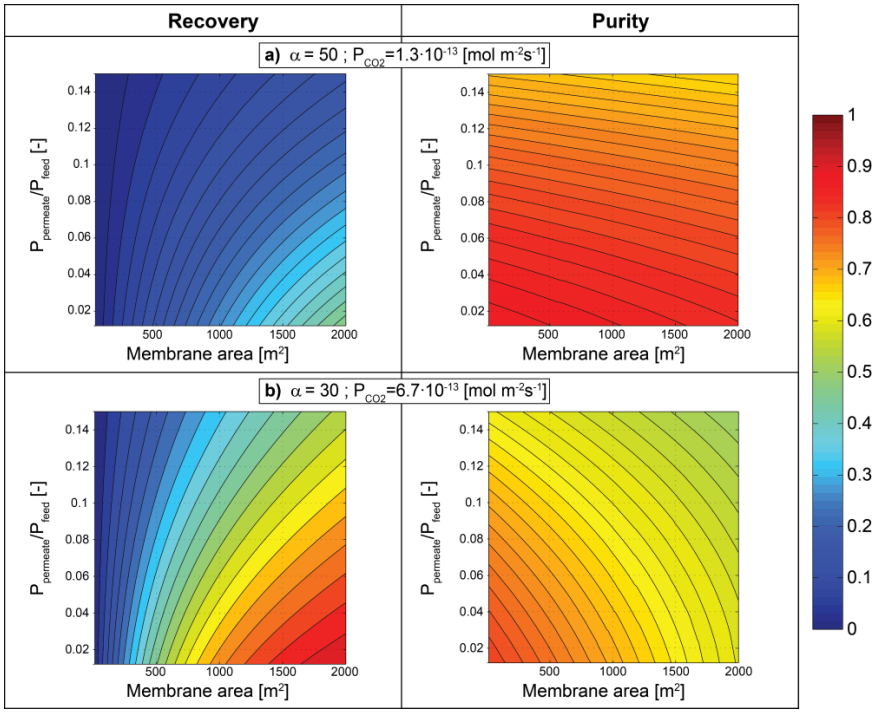

Figure 3.15: Recovery and purity maps for two single-stage configurations with α = 30 and α = 50 (corresponding permeability on the Robeson plot).

REFERENCES

1. Weller, S., Steiner, W.A, *J. Appl. Phys.*, **1950**, *21*, 279 - 283
2. Hwang, S.T., Kammermeyer, K., *Techniques of Chemistry: Membranes in Separation*, vol. VII; Wiley Interscience: New York, **1975**
3. Humphrey, J.L., Keller G.E., *Separation Process Technology*, New York: MacGraw-Hill, **1997**
4. Pan, C.Y., *AIChE J.*, **1983**, *29*, 545-552
5. Baker, R.W., *Membrane Technology and Applications*, John Wiley & Sons Ltd: United Kingdom, **2012**
6. Robeson, L.M., *Memb. Sci.*, **2008**, *320*, 390 - 400
7. Baker, R.W., Low, B.T., *Macromolecules*, **2014**, 6999 - 7013

CHAPTER 4

MEMBRANE MODULES AND PROCESSES

4.1 Membrane Modules

Membranes found their first significant application in the production of drinking water at the end of World War II. Drinking water supplies serving large communities in Germany and elsewhere in Europe had broken down, and filters to test for water safety were needed urgently. However, by 1960, although the elements of modern membrane science had been developed, no significant membrane industry existed. The seminal discovery that transformed membrane separation from a laboratory to an industrial process was the development, in the early 1960s, of the Loeb-Sourirajan process for making defect-free, high-flux, anisotropic reverse osmosis membrane [1]. With regards of gas separation, the first large scale industrial plant was applied to uranium enrichment. The separation of $U^{235}F^6$ from $U^{238}F^6$ was performed. Indeed, the molecular weight of UF^6 (uranium hexafluoride), entirely depends on the uranium isotope. $U^{235}F^6$ was enriched by using a cascade of finely micro-porous metal membranes.
In general, when dealing with real industrial applications, few key aspects must be taken into account for a membrane fabrication process to be successful:

- material with appropriate chemical, mechanical and permeation properties have to be developed.
- robust, thin, defect free membranes have to be fabricated.
- efficient, high surface area, economical modules have to be designed.

Indeed, industrial membrane plants often require a membrane area in the range of hundreds to thousands square meters to perform the separation on a commercial scale. Therefore, methods for packaging large membrane areas economically and efficiently are required. Different types of modules, depending on the different applications are used. Below, a list of the principal modules is presented.

- *Plate and Frame Membrane Modules*. They were one of the earliest types of membrane system. A schematic of a plate and frame membrane module for reverse osmosis is illustrated in figure 4.1. Membrane, feed spacers and product spacers are layered together between two end plates. The feed mixture is forced across the surface of the membrane, enters the permeate channel, and exit from a central permeate collection manifold [1]. Plate and frame units have been developed for some small-scale applications. However, they are expensive compared to alternative membrane modules, and still affected by leakages. Currently, plate and frame modules are used in electrodialysis, pervaporation and, in a limited number, in reverse osmosis and ultrafiltartion applications with highly fouling feeds. Such modules can be operated both in co- and countercurrent flow.
- *Tubular Membrane Modules*. This type of modules is characterized by a high resistance to membrane fouling, due to the good fluid hydrodynamics, i.e. turbulent flow. On the other hand, the cost is elevated due to the low surface to volume ratio. For this reason, tubular modules are nowadays limited to ultrafiltration applications, where the benefit connected to the the high resistance to

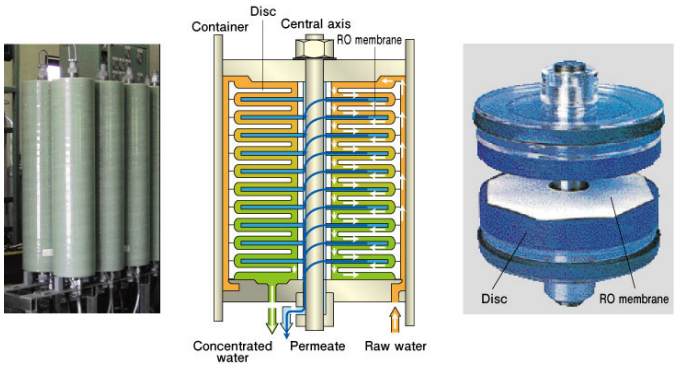

Figure 4.1: Schematic of a plate and frame module for everse osmosis, [2].

Figure 4.2: Typical tubular ultrafiltration module design, [3].

fouling outweights their high cost. Typically, the tubes consist of a porous paper of fiberglass, which serves as a support, with the membrane on the inside of the tubes, as shown in figure 4.2. In a typical tubular membrane system, many tubes are manifolded in series. The permeate is removed from each tube and sent to a permeate collection header. A drawing of a 30-tube system is shown in figure 4.3. The feed stream is pumped through all the tubes connected in series. As a consequence, it maintains a high velocity in the tubes, which helps to control membrane fouling.

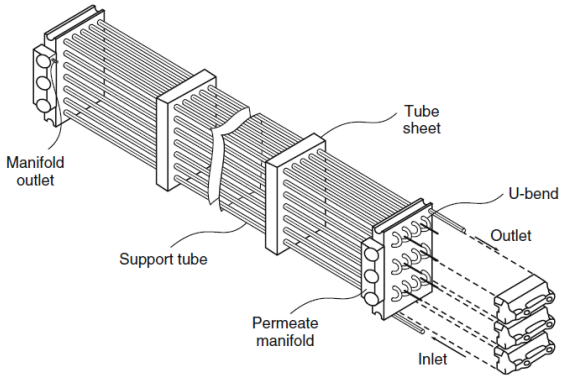

Figure 4.3: Tubular ultra-filtration system with 30 tubes connected in series, [1].

- *Spiral-Wound Membrane Modules*. Spiral-wound membrane modules were used in a number of early artificial kidney designs, and were originally developed for industrial reverse osmosis applications. Nowadays, the are used for reverse osmosis, ultra-filtration and gas separation. The design shown in figure 4.4 consists of a membrane envelope of spacers and membrane wound around a

perforated central collection tube. The feed passes axially down the module across the membrane envelope. The permeate spirals toward the center and exits through the collection tube. The module is then operated in cross-current flow.

For many years, the standard industrial reverse osmosis / gas separation spiral-wound modules had an 8 inches diameter and were 40 inches long. However, there is a trend toward increasing the module diameter. Similarly, a trend toward a higher number of envelopes is recorded. Indeed, the multi-envelope design minimizes the pressure drop encountered by the permeate fluid traveling toward the central tube, by reducing the length of the collection pipe. The approximate membrane area and number of membrane envelopes used in industrial 40 inches long spiral-wound module are reported in table 4.1, [1].

Table 4.1: typical membrane area and number of membrane envelopes for 40 inches long industrial spiral-wound modules. The thickness of the membrane spacers used for different applications causes the variation in membrane area, [1].

module diameter [in]	2	6	8	16
number of membrane envelopes	4-6	6-10	15-30	50-100
membrane area [m^2]	3-6	6-12	20-40	80-150

Four to six spiral-wound membrane modules are normally connected in series inside a tubular pressure vessel, illustrated in figure 4.5. A typical 0.2 m diameter tube containing six modules has a 150 - 250 m^2 membrane area. In general, spiral-wound modules are characterized by a fairly low manufacturing cost and a high surface to volume ratio.

- *Hollow-Fiber Membrane Modules*. Today hollow fiber membrane modules are widely used for different membrane applications. They are found in two basic geometries:

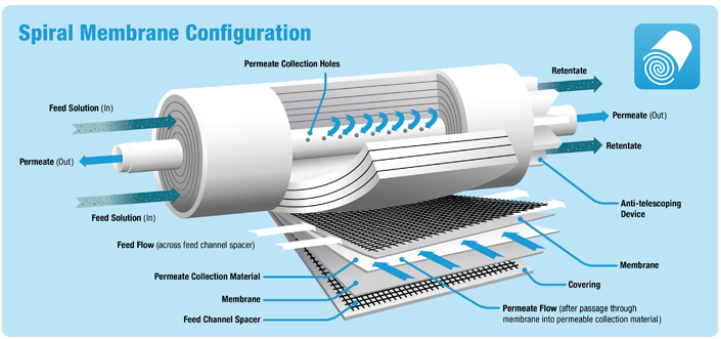

Figure 4.4: Exploded view for a spiral-wound membrane module, [4].

Figure 4.5: Typical spiral-wound module design, [5].

– The *shell-side feed* design is illustrated in figure 4.6. This geometry is used, for example, by Monsanto in their hydrogen separation systems and by Du Pont (until about 2000) in their reverse osmosis systems [1]. A loop or a closed bundle of fibers is contained in a pressure vessel. The system is pressurized from the shell side; the permeate passes through the fiber wall and exits through the open fiber ends. This design is fairly easy to make, and allows very large membrane area to be contained in an economical system. Because the fiber wall must support considerable hydrostatic pressure, the fibers usually have small diameters and thick walls, typically 50 μm internal diameter and 100 - 200 μm external diameter. This configuration is mostly used in high-pressure applications, particularly gas separation and reverse osmosis. It can be operated both in co-current and counter-current flow, with the second having a favorable partial pressure build-up (see section 3.4).

– The second type of hollow-fiber module is the *bore-side feed* type, depicted in figure 4.7. In this type of unit, the fibers are open at both ends; the feed fluid is circulated through the bore of the fibers. In order to minimize pressure drop inside the fibers, the diameters are larger than those of the fine fibers used in the shell-side feed system. This geometry is mostly used in ultra-filtration and pervaporation, mainly in co-current flow. Generally, they are operated at pressure lower than 10 bar. In bore-side feed modules, it is important to ensure that all of the fibers have identical fiber diameters and permeances, since this can significantly influence the removal achieved by the module [2]. Contrarily to the shell-side feed configuration, concentration polarization is well controlled in the bore-side feed system. Indeed, the

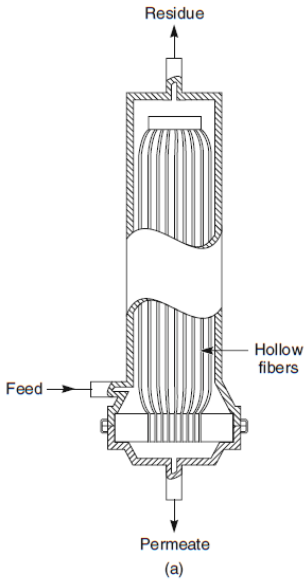

Figure 4.6: Shell-side feed design for a hollow-fiber module, [1].

feed solution passes directly across the active surface of the membrane, and no stagnant dead spaces are produced.

In general, the greatest single advantage of hollow fiber modules is the ability to pack a very large membrane area into a single module. On the other hand, bigger pressure drops are usually registered in this type of modules compared to spiral-wound configurations. The advantage in terms of membrane area can be evaluated by mean of the data provided by table 4.2, from [1].

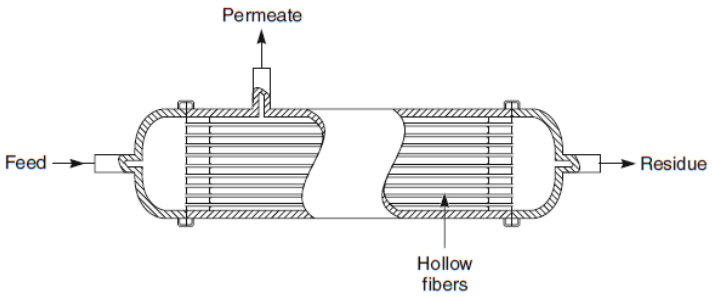

Figure 4.7: Bore-side feed design for a hollow-fiber module, [1].

Table 4.2: Effect of fiber diametr on membrane area and the number of fibers in a module of 20 cm diameter and 1 m long, [1].

Module use	High-pressure reverse osmosis and gas separation	Low-pressure gas separation		Ultrafiltration	
Fiber diameter, [μm]	100	250	500	1000	2000
Number of fibers / module, [thousands]	1000	250	40	10	2.5
Membrane area, [m^2]	315	155	65	32	16
Packing density, [cm^2/cm^3]	100	50	20	10	5

The table shows that, for the same module dimension, the hollow-fiber configuration allows around ten times the area of a spiral-wound module. As the diameter of the fibers in the module increases, the membrane area decreases. Capillary ultra-filtration modules have almost the same area as equivalent-sized spiral-wound modules.

4.2 Multistep and Multistage System Design

Because the membrane selectivity and pressure ratio achievable in a commercial membrane system are limited, a one-stage membrane system may not provide the desired separation. The problem is illustrated in figure 4.8, from [1], with the removal of a volatile organic compound (VOC), which is the most permeable component from a nitrogen feed gas.

The figure shows that 90% of the VOC in the feed stream is removed, with the permeate stream containing approximately 4% of the permeable component. Nevertheless, in many cases, 90% of removal of VOC from the feed is insufficient to allow the residue gas to be discharged, and the enrichment of the component in the permeate is also insufficient. If the main issue regards insufficient VOC removal from the feed stream, a two-step system as shown in figure 4.9 can be implemented to decrease the concentration of the permeable gas in the retentate.

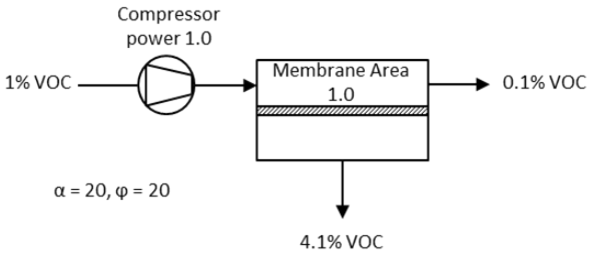

Figure 4.8: One-stage vapor separation operation. The performance of this systems was calculated for a cross-flow module using a vapor/nitrogen selectivity of 20 and a pressure ratio of 20, [1].

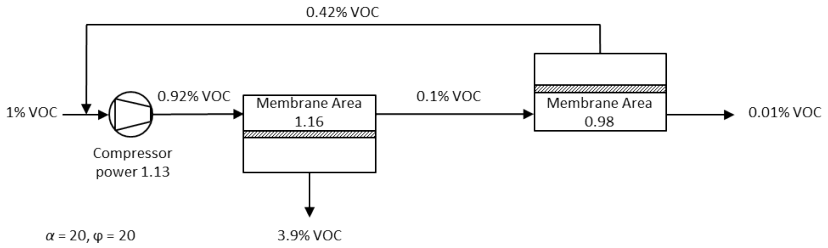

Figure 4.9: Two-stage system to achieve 99% vapor removal from the feed stream. Selectivity of 20 and pressure ratio of 20, [1].

In this two-step system, the residue stream from the first membrane unit passes across a second unit, where the VOC concentration is reduced by a further factor of 10, from 0.1% to 0.01%. Because the concentration of VOC in the feed to the second membrane unit is low, the permeate stream is relatively diluted and is recirculated to the feed stream. A multistep design of this type can achieve almost complete removal of the permeable component. However, such a removal is attained at the expense of increases in membrane area and power consumption (compression energy). As a rule of thumb, the membrane area required to remove the last 9% of a component from the feed equals the membrane area required to remove the first 90% [1].
In other cases, a 90% of removal is acceptable for the discharge stream from the membrane unit, but a higher concentration is needed to make the permeate gas usable. In this situation, a two-stage system of the type shown in figure 4.10 is exploited to enhance the concentration of the permeable gas in the permeate.

In a two-stage design, the permeate from the first membrane unit is recompressed and sent to a second membrane unit, where a further separation is performed. The final permeate is then twice enriched. In a perfectly efficient two-stage separation, the residue stream from the second stage is reduced to the same concentration of the

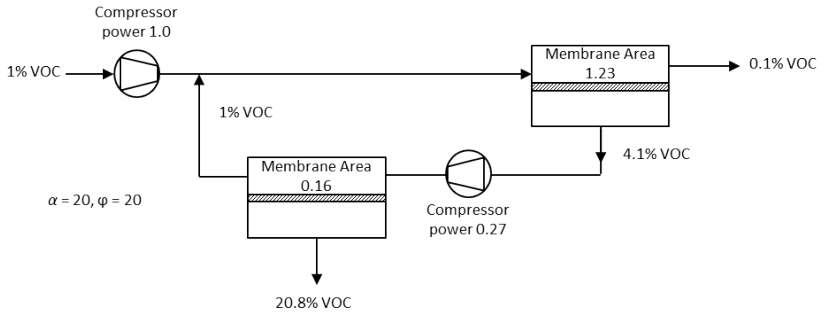

Figure 4.10: Two-stage system to produce a highly concentrated permeate stream. Selectivity of 20 and pressure ratio of 20, [1].

original stream, which represent a minimum threshold for the separation process. More complicated multistage/multistep combination processes can be designed, although seldom used in commercial systems due to their complexity. More commonly, a recycle design is used. Some example is provided in the section below.

4.3 Recycle Designs

A simple recycle design, named a two-and-one-half-stage is shown in figure 4.11 [1]. In this design, the permeate from the first membrane stage is recompressed and sent to a two-step second stage, where a portion of the gas permeates and is removed as enriched product. The remaining gas passes to another membrane stage, which brings the gas concentration close to the original feed value. The permeate from this stage is mixed with the permeate from the first stage, forming a recycle loop. By controlling the relative size of the two second stages, any desired concentration of the more permeable component can be achieved in the product.

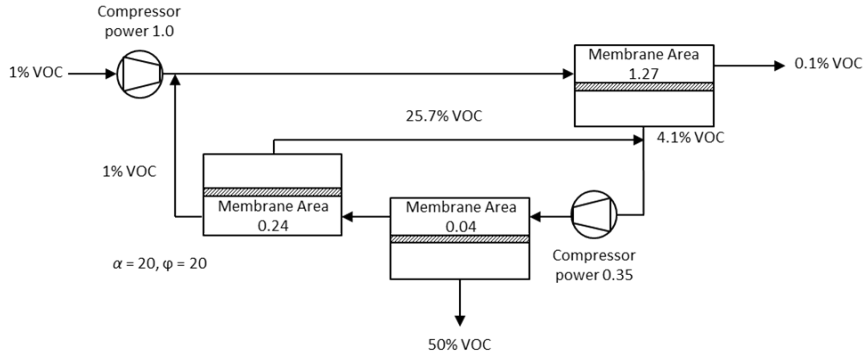

Figure 4.11: Two-and-one-half-stage system, [1].

Several types of recycle designs have been showed in literature. Although only the two-and-one-half-stage is shown here, a comprehensive analysis can be found in [1].

REFERENCES

1. Baker, R.W., *Membrane Technology and Applications*, John Wiley & Sons Ltd: United Kingdom, **2012**
2. KOBELCO ECO-SOLUTIONS CO., LTD., http : //www.kobelco − eco.co.jp/english/product/dt$_{\mathrm{m}}$odule/genri.html
3. PCI MEMBRANES, http : //www.pcimembranes.pl/A19 − A37.html
4. Membrane Technology & Research http : //www.mtrinc.com/faq.html
5. GE Power & Water, http : //www.gewater.com/products/spiral − wound − membranes.html
6. Lemanski, J.; Lipscomb, G.G., **1992**

APPENDIX A

DESIGN PROCEDURE FOR A CO-CURRENT MEMBRANE MODULE FOR GAS SEPARATION

The design procedure for a gas separation membrane module characterized by co-current flow is here outlined. Among other authors, the problem was addressed by [1] for high-flux asymmetric membranes. Figure A.1 depicts a single hollow fiber operating in co-current mode with feed flow outside the fiber, i.e. shell-side feed. The following is assumed:

- Constant membrane properties along the membrane, i.e. constant permeability and selectivity with temperature, pressure, composition.
- One dimensional (1D) model, i.e. constant concentration profiles in radial direction.
- The porous supporting layer offers a negligible resistance to the gas flow.

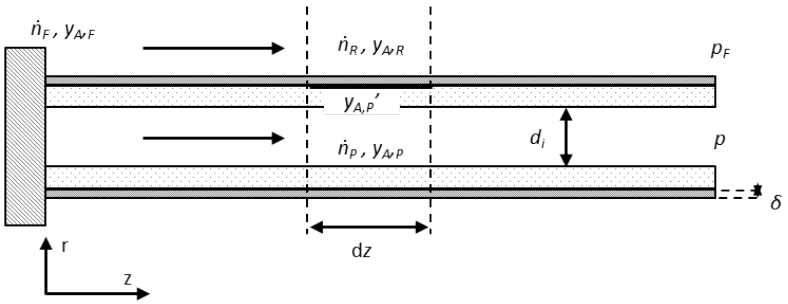

Figure A.1: Asymmetric hollow-fiber membrane operating in co-current mode with feed flow outside the fiber, [1].

- No mixing of permeate fluxes of different compositions occurs inside the porous supporting layer of the membrane (plug flow in the supporting layer).
- Isothermal process.
- Constant pressure at both sides of the membrane.
- Negligible non-idealities occurring in actual membrane separation processes: fiber deformation, non-uniform fluid distribution across the fiber bundle [2].

One of the main features of the model is that two different molar fractions for the permeate side are introduced: $y_{A,P}$ is the permeate molar fraction in the bulk phase, and $y'_{A,P}$ is the permeate molar fraction at the membrane interface. While the former depends on the flow conditions at both side of the membrane, the latter solely depends on the retentate conditions, since it is assumed the porous layer prevents any mixing at permeate side.
In the following, the retentate and permeate quantities, i.e. subscripts R and P, must be intended as referring to a generic section z along the membrane. Considering a binary mixture A + B, the following equations can be written:

- *Overall material balance equations*. The overall material balance from the feed section to a generic section z can be written by referring to the green dashed line in figure A.2.

$$\dot{n}_p + \dot{n}_r = \dot{n}_f \tag{A.1}$$

$$\dot{n}_p\, y_{\alpha,p} + \dot{n}_r\, y_{\alpha,r} = \dot{n}_f\, y_{\alpha,f} \tag{A.2}$$

  As in chapter 3, the composition equations are implied, being the two molar fractions complementary: $y_{\alpha,r} + y_{\beta,r} = y_{\alpha,p} + y_{\beta,p} = y_{\alpha,f} + y_{\beta,f} = 1$.

- *Differential material balance equations.* Material balances can be referred to the differential volumes indicated by the red dashed line in figure A.2 (retentate side), by expressing the flux across the membrane.

$$J\, ds = -d\dot{n}_r \tag{A.3}$$

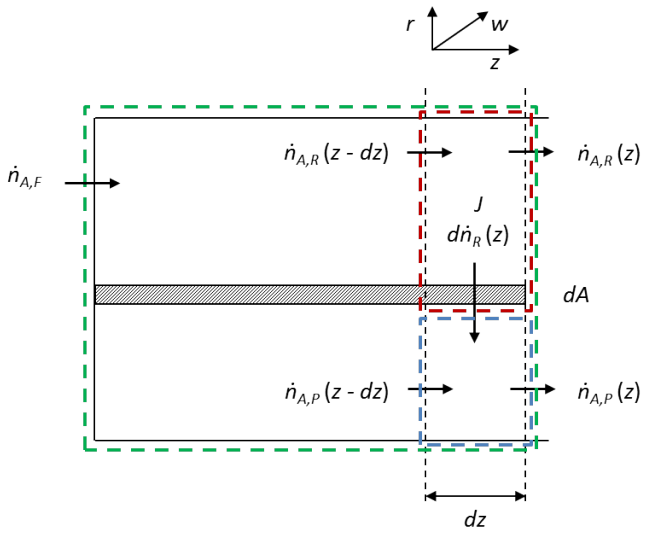

Figure A.2: Differential element dz within the co-current flow membrane module. The green dashed line represent a global material balance, while the red and blue dashed lines identify the control volumes around retentate and permeate sides, respectively.

$$J\, y'_{\alpha,p}\, ds = -d(\dot{n}_r\, y_{\alpha,r}) \tag{A.4}$$

Where the minus sign indicates that a positive flux corresponds to a reduction in the retentate flow rate, due to the material permeation across the membrane. At the same way, the differential material balances can refer to the permeate side, blue dashed line in the figure:

$$J\, ds = d\dot{n}_p \tag{A.5}$$

$$J\, y'_{\alpha,p}\, ds = d(\dot{n}_p\, y_{\alpha,p}) \tag{A.6}$$

However, it should be noted that only one couple of equations between A.3 - A.4 and A.5 - A.6 is necessary to complete the module design. In the following, equations A.3 - A.4 will be implemeneted, i.e. retentate side.

- *Flux equations*. The flux is expressed through the solution-diffusion model. Considering the flux J as a local quantity, constant within the differential element dz,

$$J\, y'_{\alpha,p} = \frac{Q_\alpha}{\delta}\, (p_f\, y_{\alpha,r} - p\, y'_{\alpha,p}) \tag{A.7}$$

$$J\, (1 - y'_{\alpha,p}) = \frac{Q_\beta}{\delta}\, \left[p_f\, (1 - y_{\alpha,r}) - p\, (1 - y'_{\alpha,p})\right] \tag{A.8}$$

The equation system composed by A.1 - A.4, A.7 - A.8, is solved to determine the performance of the membrane module. As stated in chapter 3, either the separation or the economic performance can be initially specified and the design completed accordingly. The system includes 6 linearly independent equations and 8 unknowns: $\dot{n}_r$, $\dot{n}_p$, $y_{\alpha,r}$, $y_{\alpha,p}$, $y'_{\alpha,p}$, J, p, A. The feed conditions are assumed to be given: $\dot{n}_f$, $y_{\alpha,f}$, p_f, also providing for the boundary conditions for the differential equations. The same procedure presented in section 3.3 can be applied. The only difference lays in the interpretation of $y_{\alpha,p}$ and $y'_{\alpha,p}$, defined above. As a consequence, $y_{\alpha,p}$ assumes a meaning along the whole membrane module, not only at the module output; indeed, it can be computed for a generic z through equation . A similar methodology, with few peculiarities related to the signs and the boundary conditions, can be applied to a counter-current flow membrane module.

REFERENCES

1. Pan, C.Y., *AIChE J.*, **1983**, *29*, 545-552
2. Lemanski, J.; Lipscomb, G.G., **1992**

APPENDIX B

PERMEATION UNITS AND CONVERSION FACTORS

This appendix aims at providing indications in terms of the most common gas permeation units and conversion factors.

Table B.1: Gas permeation units.

Quantity	Engineering units	Literature units	SI units
Permeation rate	Standard ft^3 / min		kmol / s
Permeation flux	ft^3 / (ft^2 day)	cm / sec (STP)	kmol / (m^2 s)
Permeability	ft^3 ft / (ft^2 day psi)	Barrers	kmol / (m s Pa)
Permeance	ft^3 / (ft^2 day psi)	Barrers / cm	kmol / (m^2 s Pa)

Table B.2: Barrers conversion factors.

Quantity	Multiply	By	To get
Permeability	Barrers	3.348 E-19	kmol / (m s Pa)
Permeability	Barrers	4.810 E-08	ft^3 (STP) / (ft psi day)
Permeance	Barrers / cm	3.348 E-17	kmol / (m^2 s Pa)
Permeance	Barrers / cm	1.466 E-06	ft^3 (STP) / (ft psi day)

Table B.3: Industry-specific gas measurements.

Industry-unit	How-measured	ft^3 / (pound mole)	kmol / msef
STP, Msef	1000 ft^3 at 32 F	359.3	1.262
Gas industry, Msef	1000 ft^3 at 60 F	379.8	1.194
Air industry, Mnsf	1000 ft^3 at 70 F	387.1	1.172